

Carolina Villarreal Lozano

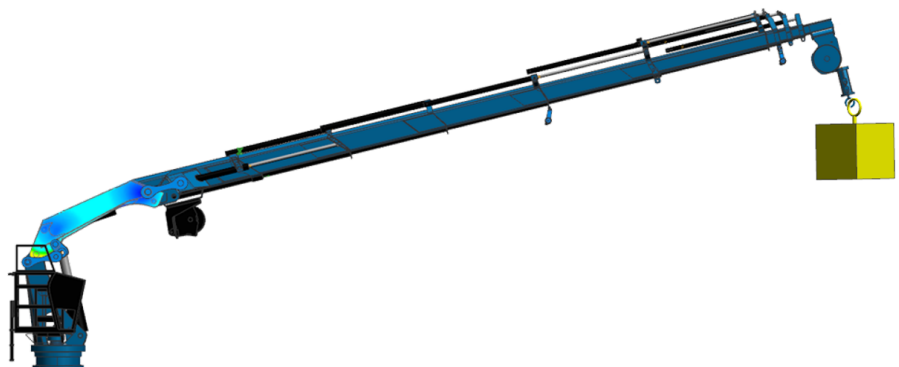
# Digital Twin for Structural Monitoring and Predictive Maintenance of a Maritime Crane

Master's thesis in Product and System Design

Supervisor: Henry Peter Piehl

June 2020

NTNU  
Norwegian University of Science and Technology  
Faculty of Engineering  
Department of Ocean Operations and Civil Engineering





---

*Life represents a progression of iterations  
in a non-stopping search  
to reach perfection.*

---

---

---



---

# Abstract

Industry 4.0 has revolutionized the industries by the application of technology in multiple ways. One of its focus is digital twins, which are virtual representations of physical products simulated in specialized software with the purpose of obtaining predictions on the product behavior. Maritime cranes are constantly exposed to severe loads, obtaining a wide range of failure modes, most related to structural factors and can be predicted by a digital twin. This project aims to develop a digital twin model to provide the crane with real-time structural monitoring that would constantly measure the structure status and loads, making possible the prediction of operations and capabilities by mixing the digital twin with data from sensors mounted in the physical crane.

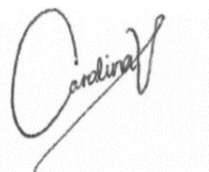
---

# Preface

The following work was planned from November 2019 and developed from January to June 2020 at the NTNU Campus Ålesund. This Master's thesis project was developed in collaboration with the project Arrowhead, and was initially defined by professor Houxiang Zhang. The project was divided in two main parts: the structural simulations, which were supervised by professor Henry Piehl. Regarding the kinematic simulations, professor Guoyuan Li was providing supervision. Professor Terje Rølvåg developed the initial 3D crane model, and additional feedback on the project.

This project represents an effort to develop and test a digital twin for a maritime crane using Siemens NX.

Ålesund, June 25, 2020.

A handwritten signature in black ink, appearing to read 'Carolina', with a long horizontal stroke extending to the right.

**Carolina Villarreal Lozano**

# Table of Contents

<b>Abstract</b>	<b>i</b>
<b>Preface</b>	<b>ii</b>
<b>Table of Contents</b>	<b>v</b>
<b>List of Tables</b>	<b>vii</b>
<b>List of Figures</b>	<b>xi</b>
<b>Abbreviations</b>	<b>xii</b>
<b>1 Introduction</b>	<b>1</b>
1.1 Motivation . . . . .	2
1.2 Background . . . . .	3
1.3 Scope . . . . .	3
1.4 Research Questions . . . . .	5
<b>2 State of the Art</b>	<b>7</b>
2.1 Digital Twin . . . . .	7
2.1.1 DT driven Product Design . . . . .	8
2.1.2 DT driven Performance . . . . .	9
2.1.3 Data Acquisition . . . . .	10
2.2 Simulation-based design . . . . .	10
2.2.1 SBD and the conventional design process . . . . .	11
2.2.2 Accuracy of the SBD numerical predictions . . . . .	12
2.2.3 SBD using Siemens NX . . . . .	13
2.3 Structural Analysis by the Finite Element Method . . . . .	15
2.3.1 Finite Element Method . . . . .	17
2.4 Maintenance and Monitoring . . . . .	18
2.4.1 Preventive Maintenance . . . . .	19

---

2.4.2	Predictive Maintenance . . . . .	19
2.5	Structural Analysis & Maintenance-Monitoring . . . . .	20
2.5.1	Structural Health Monitoring . . . . .	20
2.5.2	Maritime Structures and Ship Monitoring Systems . . . . .	21
2.5.3	Bridge Monitoring Systems . . . . .	22
2.6	Digital Twin & Structural Analysis . . . . .	23
<b>3</b>	<b>Methodology</b>	<b>25</b>
3.1	Study Case . . . . .	25
3.1.1	Assumptions . . . . .	26
3.1.2	Limitations . . . . .	27
3.2	Research Method . . . . .	28
3.3	Main model preparation . . . . .	28
<b>4</b>	<b>Structural Simulation</b>	<b>33</b>
4.1	Model selection and considerations . . . . .	34
4.2	Mesh convergence study . . . . .	35
4.3	Validation tests . . . . .	38
4.3.1	Revolute joint . . . . .	38
4.3.2	Slider joint . . . . .	41
4.3.3	Hydraulic cylinders . . . . .	45
4.3.4	Geometry Idealization . . . . .	50
4.3.5	Validation tests conclusion . . . . .	50
4.4	Tests using Finite Element Method . . . . .	50
4.4.1	3D Elements . . . . .	51
4.4.2	2D Shell Elements . . . . .	54
4.4.3	1D Beam Elements simplification . . . . .	54
4.5	Results summary . . . . .	56
4.6	Suggested strain gauge sensor locations . . . . .	57
4.7	Flexible Body Sim and preparation for the Digital Twin . . . . .	58
<b>5</b>	<b>Kinematic Simulation</b>	<b>61</b>
5.1	Model selection and considerations . . . . .	62
5.1.1	Crane Joints . . . . .	62
5.2	Crane Operation . . . . .	63
5.3	Motion model setup . . . . .	64
5.3.1	Motion Bodies . . . . .	64
5.3.2	Joints . . . . .	64
5.3.3	Drivers . . . . .	65
5.3.4	3D Contact . . . . .	67
5.4	Motion control and preparation for the Digital Twin . . . . .	67
5.4.1	List of inputs for the motion sim . . . . .	68
5.4.2	Simulation of Data Input . . . . .	68
5.4.3	2D Profile control . . . . .	69
5.5	Sensor locations . . . . .	70
5.5.1	List of sensors and plots in Data Output . . . . .	70

---

---

5.5.2	Excel spreadsheet output . . . . .	70
5.6	Results summary . . . . .	71
5.6.1	Revolute joints . . . . .	72
5.6.2	Slider Joints . . . . .	73
5.6.3	Load and Hook sensors . . . . .	74
5.6.4	Cylinders . . . . .	75
5.6.5	Motion Envelope . . . . .	75
<b>6</b>	<b>Digital Twin</b>	<b>77</b>
6.1	Connecting the structural and kinematic simulations . . . . .	77
6.2	Results . . . . .	78
6.2.1	Displacement . . . . .	78
6.2.2	Stress . . . . .	79
6.3	Smart Controller . . . . .	80
<b>7</b>	<b>Further work</b>	<b>83</b>
<b>8</b>	<b>Conclusions</b>	<b>85</b>
	<b>References</b>	<b>87</b>
	<b>Appendix</b>	<b>91</b>
8.1	Structural Simulation with 5 kN . . . . .	91
8.1.1	3D Partial Test . . . . .	91
8.1.2	3D Complete Test . . . . .	93
8.1.3	1D Square cross-section test . . . . .	94
8.1.4	1D Real cross-section test . . . . .	94
8.1.5	Results . . . . .	95
8.2	Kinematic Simulation . . . . .	95
8.2.1	List of sensors . . . . .	95

---

---

# List of Tables

2.1	Finite Element Types . . . . .	18
3.1	Bill of materials of the initial 3D model . . . . .	26
3.2	Palfinger PK-65002-M operational specifications [1] . . . . .	27
3.3	Palfinger PK-65002-M detailed lifting capacity [1] . . . . .	27
3.4	Crane dead weight comparison test . . . . .	28
3.5	List of joints with the expression name and limits as used in NX . . . . .	29
4.1	Mesh Convergence Analysis for the structural parts 1-6 . . . . .	36
4.2	Mesh Convergence Analysis for the structural parts 7-13 . . . . .	37
4.3	Results for revolute joint validation tests . . . . .	40
4.4	Results for slider joint validation tests . . . . .	45
4.5	Results for the hydraulic cylinder test . . . . .	49
4.6	Results for partial tests at 20 kN . . . . .	53
4.7	Results for complete tests at 20kN . . . . .	53
4.8	Results for complete 1D tests at 20kN . . . . .	56
4.9	Structural simulation test results summary for 20 kN . . . . .	57
5.1	Simulation time using different crane hooks and 3D contact . . . . .	67
5.2	List of inputs for the motion simulation using a Profile 2D control . . . . .	68
8.1	Results for 3D partial tests at 5 kN . . . . .	92
8.2	Results for 3D complete tests at 5 kN . . . . .	94
8.3	Structural simulation test results summary for 5 kN . . . . .	95
8.4	List of sensors and plots for the revolute joints . . . . .	95
8.5	List of sensors and plots for the slider joints . . . . .	96
8.6	List of sensors and plots for the additional sensors . . . . .	97

---



# List of Figures

1.1	NTNU Gunnerus ship depiction of a digital twin [2]	2
1.2	Palfinger crane PK-65002-M mounted in the NTNU Gunnerus ship	3
1.3	Digital twin scope using the NTNU Gunnerus ship	4
1.4	Research Venn Diagram	4
2.1	Siemens aircraft fuel system digital twin [3]	8
2.2	SBD applied to ship hull design optimization [4]	11
2.3	Design processes comparison	12
2.4	Tools for SBD using Siemens NX	13
2.5	NX Modeling displaying the maritime crane assembly with a highlighted part	13
2.6	NX FEM displaying a crane part with a tetrahedral mesh	14
2.7	NX Simulation output	14
2.8	NX Motion showing the different menus	15
2.9	NX Motion showing an animation	15
2.10	Degrees of freedom of a rigid body in space	16
2.11	Revolute and slider joints	16
2.12	Different maintenance approaches [5]	18
2.13	Maintenance costs plot [5]	20
2.14	Typical Hull Monitoring System for a Bulk Carrier [6]	21
2.15	Structural Monitoring of the Akashi Kaikyo bridge [7]	22
3.1	Initial 3D model of the Palfinger crane	25
3.2	3D model of the Palfinger crane highlighting structural components	26
3.3	Simulation models	28
3.4	Crane joints	29
3.5	Gap between the telescopic parts	30
3.6	Defining the joint limits for a Hinge or Revolute joint in NX for <i>RevAngle2</i>	30
3.7	List of expressions programmed in NX	31
4.1	Simulation-based design diagram for the structural simulation	33

---

4.2	Progression of the tests . . . . .	34
4.3	Degrees of freedom for the structural analysis simulation . . . . .	34
4.4	Partial and complete models, showing the boundary conditions . . . . .	35
4.5	Mesh size comparison for part 3 using <i>CTetra(10)</i> , displaying displacement results . . . . .	37
4.6	Validation tests for the structural simulation . . . . .	38
4.7	Pinned constraint for the revolute joint test . . . . .	39
4.8	C-Beam with RBE3 connector for the revolute joint test . . . . .	39
4.9	Fixed constraint for the revolute joint test . . . . .	40
4.10	Mesh mating for the sliding joint test . . . . .	41
4.11	Mesh mating adding irregular material between the parts . . . . .	42
4.12	RBE3 connection for the sliding joint test . . . . .	42
4.13	Surface to surface gluing method for the sliding joint test . . . . .	43
4.14	Surface to surface gluing: visualization of the material or <i>glue</i> force results . . . . .	43
4.15	Unsuccessful contact convergence plot for the surface to surface contact method . . . . .	44
4.16	Hydraulic cylinders . . . . .	45
4.17	Hydraulic cylinders modeled as <i>superelements</i> , displayed as solids in NX FEM . . . . .	46
4.18	Revolute model without hydraulic cylinders . . . . .	46
4.19	Revolute model with hydraulic cylinders . . . . .	47
4.20	Partial model without hydraulic cylinders . . . . .	47
4.21	Partial model with hydraulic cylinders . . . . .	48
4.22	Complete model without hydraulic cylinders . . . . .	48
4.23	Complete model with hydraulic cylinders . . . . .	49
4.24	Stress plot of the complete model with the cylinders (hidden) . . . . .	49
4.25	Real model and the idealized part model . . . . .	50
4.26	Test plan for the structural simulation . . . . .	51
4.27	3D Real Model - Partial Test at 20 kN result . . . . .	51
4.28	3D Ideal Model - Partial Test at 20 kN result . . . . .	52
4.29	3D Real Model - Complete Test at 20 kN result . . . . .	52
4.30	3D Ideal Model - Complete Test at 20 kN result . . . . .	53
4.31	2D Shell of the crane . . . . .	54
4.32	1D model using the solid visualization in comparison with the 3D real model . . . . .	54
4.33	1D approximation models with different cross-sections . . . . .	55
4.34	1D square cross-section approximation test results at 20 kN . . . . .	55
4.35	1D real cross-section approximation test results at 20 kN . . . . .	56
4.36	Suggested strain gauge locations and stress plots in a front perspective . . . . .	57
4.37	Suggested strain gauge locations and stress plots in a top perspective . . . . .	58
4.38	NX FEM model with the assembly points for a flexible body simulation . . . . .	59
4.39	NX Sim results showing a set of result modes for the same part . . . . .	59
5.1	Simulation-based design diagram for the kinematic simulation . . . . .	61
5.2	Kinematic Model . . . . .	62
5.3	Joints for the kinematic model . . . . .	62
5.4	Test scenario for the kinematic simulation . . . . .	63

---

---

5.5	Joint limit configuration for the <i>link1</i> slider . . . . .	65
5.6	Harmonic Driver setup for a revolute joint . . . . .	65
5.7	Joints test . . . . .	66
5.8	Driver setup for all variables programmed using NX expressions . . . . .	66
5.9	Initial hook model and improved version, to reduce the 3D contact computation time . . . . .	67
5.10	Screenshot from the Excel spreadsheet for the data input . . . . .	69
5.11	2D Profile Driver configuration window for <i>Angle1</i> . . . . .	69
5.12	Location of sensors in the crane . . . . .	70
5.13	Excel Output File with measurements from 50 sensors . . . . .	71
5.14	Kinematic Simulation of the maritime crane using NX Motion . . . . .	71
5.15	Revolute joints plot during the kinematic simulation . . . . .	72
5.16	Crane angle . . . . .	72
5.17	Linear displacement test for the slider joints . . . . .	73
5.18	Force plot for the slider joints . . . . .	73
5.19	End effector position plot . . . . .	74
5.20	Hook cable displacement . . . . .	74
5.21	Forces in the revolute angles, also considered as forces in the cylinders . . . . .	75
5.22	Motion envelope of the kinematic simulation . . . . .	75
6.1	Screenshot of the Digital Twin simulation visualizing the displacement at 56 seconds . . . . .	78
6.2	Screenshot of the Digital Twin simulation visualizing the displacement at 254 seconds . . . . .	78
6.3	Screenshot of the Digital Twin simulation visualizing stress at 186s . . . . .	79
6.4	Screenshot of the Digital Twin simulation visualizing stress at 441s . . . . .	79
6.5	Digital Twin defining the sensor data input and control output . . . . .	80
7.1	Goal of the digital twin for the maritime crane . . . . .	83
8.1	3D Real Model - Partial Test at 5 kN result . . . . .	91
8.2	3D Ideal Model - Partial Test at 5 kN result . . . . .	92
8.3	3D Real Model - Complete Test at 5 kN result . . . . .	93
8.4	3D Ideal Model - Complete Test at 5 kN result . . . . .	93
8.5	1D square cross-section approximation test results at 5 kN . . . . .	94
8.6	1D real cross-section approximation test results at 5 kN . . . . .	94

---

# Abbreviations

<b>DM</b>	=	Digital twin
<b>IoT</b>	=	Internet of Things
<b>PM</b>	=	Predictive Maintenance
<b>PP</b>	=	Physical product
<b>VM</b>	=	Virtual model
<b>SM</b>	=	Structural monitoring
<b>SBD</b>	=	Simulation-based design
<b>CPS</b>	=	Cyber-physical systems
<b>NTNU</b>	=	Norwegian University of Science and Technology
<b>CAD</b>	=	Computer-Aided Design
<b>FEM</b>	=	Finite Element Method
<b>FEA</b>	=	Finite Element Analysis
<b>DOF</b>	=	Degrees of Freedom
<b>SHM</b>	=	Structural Health Monitoring

# Introduction

Industry 4.0, also called 'the fourth revolution' has become a trending topic in the industries together with the internet of things and digital twin technologies due to the promising benefits. The internet of things is capable of communicating smart devices to allow the data exchange through internet, [8], and it enables the retrofit of existing assets with sensors in order to make them smart and connect them to the cloud, granting the possibility of an integration between the physical and virtual world. Digital twins are capable of predicting the behavior of a product through a connection of a real product to its computational model or simulation, defined as physical product and virtual model.

The capability of a digital twin system to predict its behavior opens the door to new possibilities such as predictive maintenance, which by the use of sensors in the physical product, is able to detect the status of the critical components and together with the data measured, estimates how much time is available before the next service. Then the digital twin supports by locating the components that need to be fixed using the virtual model display with technical data. This will allow the operators to understand exactly where the part that needs repair is located and how to reach it, reducing the maintenance downtime.

The information gathered from the sensors in the physical product can also be used as input for the virtual model, which is able to simulate and display in form of graphics and visualizations how the product would react to specific conditions or situations. For example, in the case of a maritime crane, this could help the operators to support their decision-making processes with a visualization of the possible scenario if a certain operation was executed. The information used to predict scenarios is gathered from the sensors and taken in real-time into the virtual counterpart of the digital twin, to simulate it. The worst case scenarios of the structure can even be simulated in the development stages and programmed to be avoided in the control system, in order to protect the equipment.

All these technological advances are now possible as a result of the price decline of the advanced computational and electronic equipment.[9] At the same time, the computer ca-

pabilities have increased, now being able to run more complex software and simulations. This opens new opportunities such as simulation-based design, which is an iterative design methodology that uses the output information from simulations to improve the product design and validation.

The NTNU has been working on developing a digital twin system of the Gunnerus ship, presented in **Figure 1.1**. Currently the digital twin is able to simulate trips, calculating the fuel consumption while gathering historical data from the sensors. During the last summer the thrusters were added to the simulation with successful results.



**Figure 1.1:** NTNU Gunnerus ship depiction of a digital twin [2]

This master thesis aims to explore and develop the digital twin of a maritime crane involving structural and kinematic analysis by applying simulation-based design with the purpose of testing the possibility of providing real-time structural monitoring and predictive maintenance. The expected outcomes of this project are to obtain the first digital twin of a maritime crane, being capable of providing structural monitoring and maintenance capabilities. This project has been developed in collaboration with the project Arrowhead. The success of the project depends on the accuracy, detail level and computational effort of the models. [10]

## 1.1 Motivation

The digital twins for the maritime industry, specifically cranes, are still in the research stage and there are very few applications reported that contain structural monitoring and predictive maintenance. The benefits of having a digital twin that is able to monitor the current status or future operation cases of the crane, extend from increasing the safety in the operations, to reducing maintenance downtime and adding decision-making capabilities. In addition, the connection of real-world products and simulations using computational technology are very promising and open a great amount of possibilities, many of those are yet to be discovered.

## 1.2 Background

Maritime cranes are constantly subjected to severe loads, which result in a wide range of failure modes. Usually the issues are detected by condition monitoring, which means that it is detected when the item is already having operational problems or damaged, and since it happens unexpectedly, it takes time to locate the damaged component and fix it. Most of the failures are related to structural factors, and can be predicted by a digital twin with structural monitoring.

The objective is to develop a digital twin to equip the maritime crane with real-time structural monitoring, constantly measuring the structure status, making possible the prediction of operations and capabilities using the virtual model together with data from sensors mounted in the real crane or physical product. The crane that will be studied in this project is a Palfinger PK-65002-M. The physical twin of this crane is mounted in the NTNU Gunnerus ship and can extend up to 20.4 meters with a maximum lifting capacity of 22,000 kilograms, and is displayed in **Figure 1.2**.



**Figure 1.2:** Palfinger crane PK-65002-M mounted in the NTNU Gunnerus ship

## 1.3 Scope

Since the topic digital twin is very broad, the definition approached in this master thesis project is represented in **Figure 1.3**, defining the digital twin as a closed loop system between the physical product and the virtual model, connected through a sensor data input obtained from the sensors mounted in the physical product, which will serve as a simulation input for the virtual model. From this connection, a control output or feedback will

be connected to the physical product, providing increased safety.

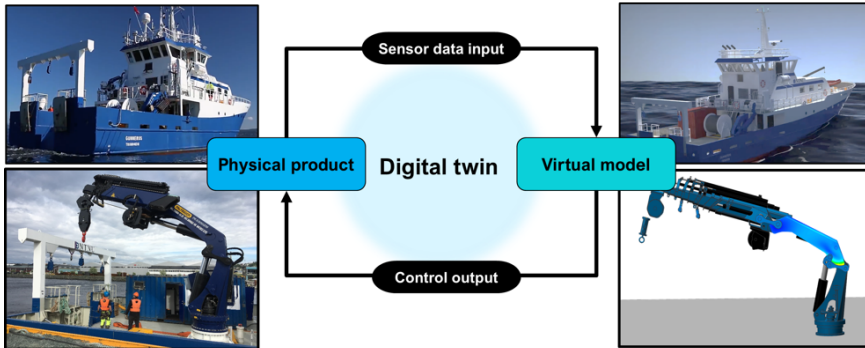


**Figure 1.3:** Digital twin scope using the NTNU Gunnerus ship

As an example using the maritime crane, the physical twin sends the sensor current status such as joint positions and structural loads to the virtual twin, which is able to simulate the current and future conditions, and if it detects a risk situation, the control output will stop or limit the operation ranges in order to protect the equipment and the crew.

Considering the previous definition, this project will explore the possibilities of the digital twin in the maritime industry, particularly in a maritime crane. This virtual model considers both the structural and the kinematic simulations, which are developed by applying simulation-based design. Therefore, the three main research topics for this project are digital twins, structural analysis and simulation-based design, shown in **Figure 1.4**.

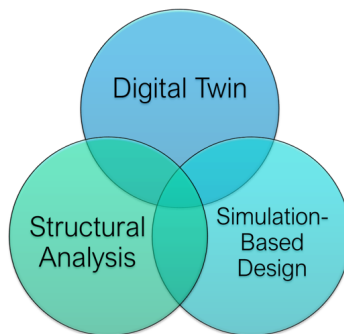


**Figure 1.4:** Research Venn Diagram



## 1.4 Research Questions

In the course of this master thesis the previous topics will be explored with the objective of answering the following questions:

1. Which computational methods can be used to create a crane-simulation model, both for kinematics and finite element analysis?
2. How can a virtual model be created keeping the balance between accuracy and computational efficiency?
3. How can simulation-based design be used to find the optimal sensor placement?
4. Which data is required for designing a smart controller?



# State of the Art

## 2.1 Digital Twin

The very first definition of a digital twin was developed by the NASA in 2012 and was defined as *"an integrated multi-physics, multi-scale, probabilistic simulation of an 'as-built' vehicle or system that uses the best available physical models, sensor updated, fleet history, etc... to mirror the life of its corresponding flying twin."*, first used in the Aerospace Industry with the objective of detecting structural anomalies.[11] The evolution of the digital twin concept has been changing over the years, adjusting to the technology capabilities.

Siemens, a high-technology company which is driven by digitalization, defines the term digital twin as *"a virtual representation of a product or process, used to understand and predict the physical counterpart's performance characteristics"* [12] and they are used in the industry as a tool to predict and optimize products, even before the investments are made. They increase the possibilities for testing a new product, and it doesn't require any physical prototype.

Digital twins are a closed loop systems between a physical product which has connected sensors that transmit the status data as inputs in the virtual model. The methods they use to maintain a high accuracy are an accurate virtual model which is capable of running real-time calculations, allowing a continuous monitoring of the product.

In a more recent paper, the digital twin concept is taken further by adding simulations. It is defined as *"A comprehensive digital representation of an individual product, which includes the properties, condition, and behavior of the real-life object through models and data. It is a set of realistic models that can be used to simulate its current behavior in the selected environment."*[13] This means that the digital twin model must be accurate and precise in representing its physical counterpart. The virtual model of a digital twin must be designed with the correct dimensioning, assembly constraints and movement ranges. In addition to the material specifications and the parameters for the actuators. The digital

twin concentrates all the information under one model, and can be used to simulate in any required environment.

In [3], Siemens Software developed a digital twin for an aircraft fuel system, as displayed in **Figure 2.1**. This model was developed using NX Simcenter, and the physical model has a series of actuators and sensors that are connected to the digital twin.

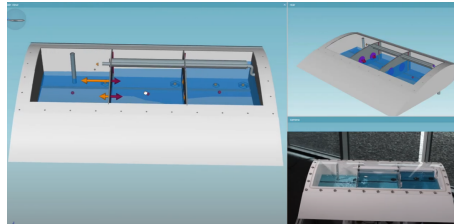


**Figure 2.1:** Siemens aircraft fuel system digital twin [3]

According to [14], a digital twin has three main characteristics, which are:

1. **Modularity**

Designing products and processes in a modular way, provide an increased efficiency when building up a digital twin model.

2. **Connectivity**

The connectivity is achieved using internet of things in every module, enabling monitoring and control of the systems.

3. **Autonomy**

Autonomy refers to efficient decision-making capabilities of the system.

There are several types of digital twins, [12; 15] they are classified according to the stage of the product life-cycle they are applied to, such as DT-driven product design, manufacturing and performance. The most relevant digital twin types according to this project will be explained in detail.

### 2.1.1 DT driven Product Design

The objective of this type of digital twin is to simulate and predict how a product behaves in the real world. It also works for validating the performance of a product in several conditions, making the design process an iterative virtual simulation, reducing the need of physical prototypes. Based on digital twins, it consists of three stages [15]:

1. **Conceptual Design**

Most important design phase, where all the requirements data is gathered. By applying the digital twin in this phase, all the information can be integrated and the customers feedback can be made more transparent since the virtual model is a true copy of the physical. This facilitates the product evolution.

## 2. Detailed Design

During this stage, the design is completed and the prototype is constructed. For this stage, several iterations of simulations are required to ensure the product performance. If the digital twin technology is considered, the physical prototype can be used as the real part, together with the virtual representations many different scenarios can be tested.

## 3. Virtual Verification

Instead of running a traditional batch production, using a digital twin can predict if there are design defects and display the causes. In this stage, the product design can be tested in realistic scenarios and particular operations, to accurately predict the performance.

### 2.1.2 DT driven Performance

The objective of this digital twin is to capture, analyze and act in an automated-way according to a set of established programming decisions. It is called performance because the decisions taken are according to the best achievable performance and it is applied to complex products. *"Aircrafts, vehicles and electric equipment are characterized by complex structures, multiple parts, and inconsistent degradation of the material function, and any of these may lead to product malfunction and/or serious safety accidents."* [15].

In this case, there are nine different performance services that can be applied with the digital twins [15], detailed as following:

#### 1. Real-time monitoring

This is the most used service, consisting of applying advanced sensing and data transfer in the physical product with the objective of keeping the digital twin updated. Some examples for the real-time transferred variable are: a position, energy consumption, user operation data, wear and loads received.

#### 2. Energy consumption prediction

By applying statistics in the historical data, this digital twin can predict and provide accurate forecasts, leading to a considerable reduction in energy consumption.

#### 3. User behavior analysis

By keeping historic data of the operation habits of a machine or system, the data and techniques of the users can be tracked and used to improve the training and define best practices, even identifying areas to automate.

#### 4. Operation guide

The operation of a product can be trained virtually and operational errors can be corrected in real-time if a failure was detected in the virtual digital twin system, with the purpose of protecting the equipment, and user learning.

#### 5. Optimization

By keeping historic data of the operation habits, the programming and control of the product can be upgraded to be made easier, error-proof and faster.

**6. Failure Prediction**

By using material properties in the virtual model and structural analysis, failure modes can be predicted, communicated in advance to users, and even avoided with programming.

**7. Product Maintenance**

When a technical problem arises, by using the virtual model it is much easier to detect the location, part and technical specifications of the items to replace and dis-assembly sequence, reducing maintenance time and downtime.

**8. Virtual Maintenance**

By using augmented reality and physical tools such as tablets or smart glasses to display the digital twin, the users can get the overview or a training before they execute the maintenance. As a consequence, the repairing accuracy and downtime are reduced.

**9. Virtual Operation**

The virtual model offers the possibility of providing virtual training, shortening the real-product training while improving the accuracy, reducing risks. This type of technology is already applied in the Offshore Simulator Centre.[16]

Applying the digital twin principle during the operation opens the door to a great number of possibilities that reduce risks, costs and improves the efficiency in several ways. For this project, the performance services that will be developed are real-time monitoring and failure prediction as a first step. The digital twin developed in this project can be further improved to provide training and product maintenance applications.

### **2.1.3 Data Acquisition**

Data acquisition is a crucial part for successfully implementing digital twins, which require continuous data flow across several platforms. Digital twins are much more effective if the data is transmitted in real-time and if there is access to a historic database. For these operations, a specialized system or software is required, together with interfaces.[17]

For this project, the digital twin will be designed to receive the signals from the sensors mounted in the physical crane, measuring joint positions. To test this, the data will be simulated using a spreadsheet with values of these variables.

## **2.2 Simulation-based design**

Simulations are key tools used in several fields with the purpose of understanding the factors that control the behavior of a system, in order to do accurate predictions, allowing the identification of possible improvements to achieve the desired performance [18]. Particularly in the product design process, simulations have a huge impact in minimizing costs,

detecting errors and enabling product optimization.

Simulation-based design was developed during the 2000s in the shipbuilding industry, well-known for developing almost unique complex products and having no opportunity of design iterations [19]. The purpose SBD originally was to reduce the ship development time, optimize the design and product efficiency. One of the most used test scenarios in this industry is the ship hull design optimization, by evaluating hydrodynamic performance with a computational fluid dynamics (CFD) module, shown in **Figure 2.2**. The ships are verified and tested digitally during several design stages and scenarios.

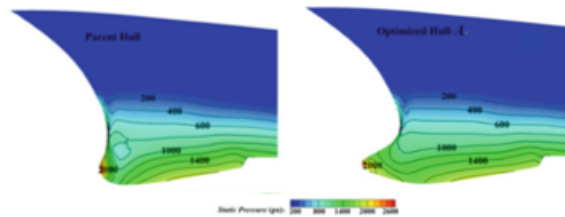


**Figure 2.2:** SBD applied to ship hull design optimization [4]

Nowadays, SBD has spread across diverse industries and successfully integrates multiple disciplines among mechanical engineering, mechanics, computer science, materials and physics for the simulation stages, contributing with innovative and accurate virtual prototyping. [20]

### 2.2.1 SBD and the conventional design process

SBD is an iterative method which verifies and optimizes a product behavior by the use of simulations, and by analyzing the results, provides feedback to the design process with the objective of identifying opportunity areas such as possible design failures, cost reduction possibilities, and product optimization. SBD is able to simulate the product life-cycle steps, such as design, manufacturing, testing, operation and maintenance by using 3D simulation techniques in a virtual environment [21]. The computational technology has been evolving fast, now making possible the virtual prototyping of products in a efficient and reliable way. [22].

The contrast from a conventional design process and SBD is shown in **Figure 2.3**. Conventional design processes, displayed in **Figure 2.3a** are straightforward and go from design to simulation of the product and conditions, to the verification stage, where this tool is only used as a performance-check. The SBD process in **Figure 2.3b** is a cycle of iterative improvements, where once the initial design and simulation is done, the results are verified and then improvement aspects will be mapped out and used as input for the design. The iterations can last until the product has been optimized enough to meet the design criteria,

or in research cases, to find the optimal conditions and best practices.

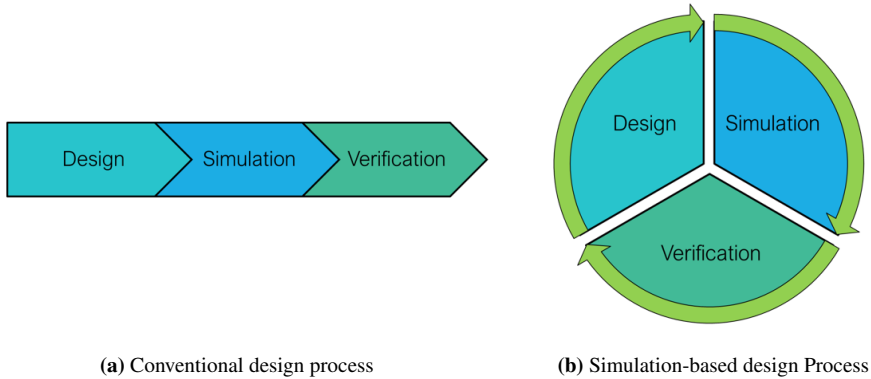


**Figure 2.3:** Design processes comparison

As observed in **Figure 2.3b**, SBD has three stages[23]:

1. **Design**

The design phase consists of creating the product model and detailing the geometry. This phase considers the necessary simplifications for simulation performance, such as the removal of complex features, or creation of the idealized parts.

2. **Simulation**

This phase considers all the necessary steps be able to run a simulation, such as meshing, application of boundary conditions, to solving the model with the software, which is a process that is done automatically by the computers.

3. **Verification**

Verification is the task of analyzing the simulation results, understanding the product behavior and gathering information for improving the design. This phase provides new parameters and numerical predictions to use as input in the next design iteration.

## 2.2.2 Accuracy of the SBD numerical predictions

Every iteration of the SBD is able to generate predictions about the product behavior, but the accuracy of these numerical predictions depends directly on the following requirements: [4]

1. **Rapidity**

The simulation must preferably perform the calculations quickly, since it will be constantly used along the iterations. This requirement depends strongly on the computational specifications and hardware.



## 2. Accuracy

The accuracy of the designed model and simulation will have a strong impact on the quality of the optimizations. Meaning that if the initial model or the simulation parameters are not defined correctly, the quality of the output will be compromised.

## 3. Sensitivity

The simulation method and model should be sensitive enough to recognize small changes done to the design or parameters, and display different results.

### 2.2.3 SBD using Siemens NX

The software used to develop the crane virtual twin is Siemens NX, particularly the version 1892, which was recently released. This software is among the most advanced that already integrates product design, assembly, manufacturing, and several types of specialized simulations such as finite element analysis, thermal, acoustic and motion analysis, among many others.

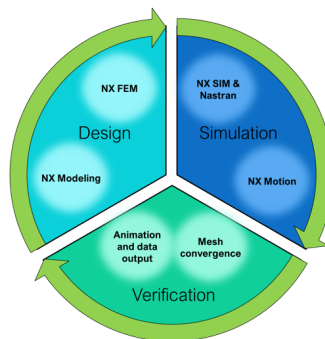


**Figure 2.4:** Tools for SBD using Siemens NX

As displayed in **Figure 2.4**, for this project, the following NX modules will be used:

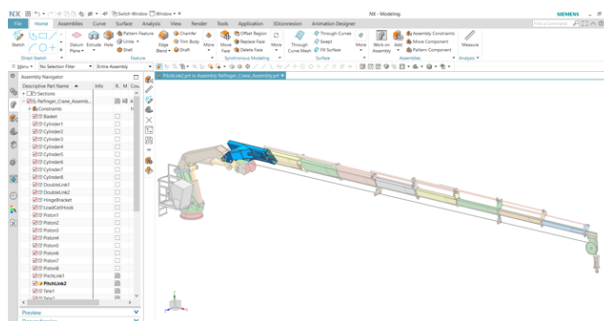


**Figure 2.5:** NX Modeling displaying the maritime crane assembly with a highlighted part

- **NX Modeling**

This module covers all the design features, constraining, and assembly analysis. It allows the user to create the parts, and modify them easily even within an assembly, as shown in **Figure 2.5**. With the flexibility of this module, the re-design phase for every SBD iteration becomes fast.

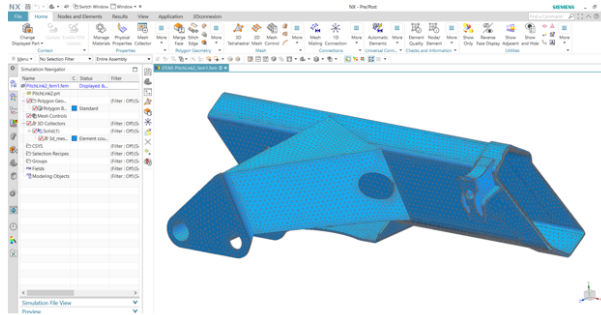


**Figure 2.6:** NX FEM displaying a crane part with a tetrahedral mesh

- **NX FEM**

The finite element method module allows the design of the meshes, setting up materials and defining the unions. It allows the user the analysis using 1D, 2D and 3D elements. **Fig 2.6** shows a crane part with a 3D tetrahedral meshing.

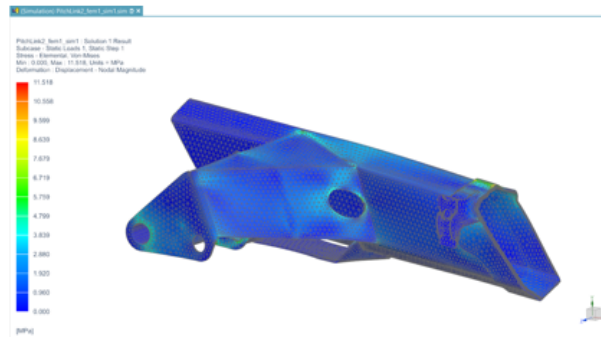


**Figure 2.7:** NX Simulation output

- **NX Nastran Simulation**

NX simulation is used for the definition of the boundary conditions such as forces and constraints for the structural analysis, and it takes as mesh source the NX FEM part. The solver in the background is NX Nastran, and it can be configured to obtain particular results such as force, contact, and gluing options. **Figure 2.7** shows the stress results of a structural analysis in a crane part. [24]

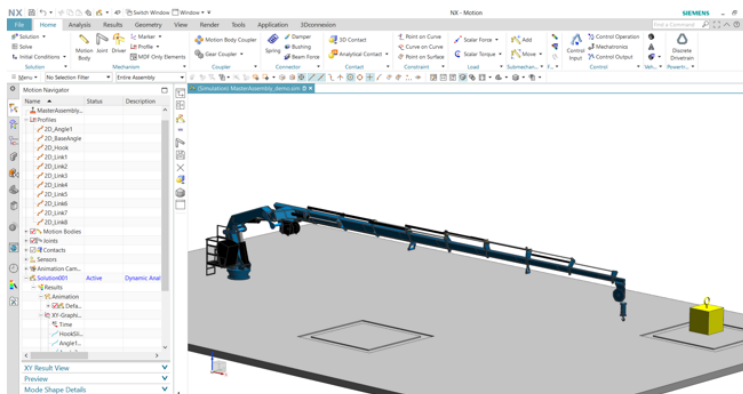


Figure 2.8: NX Motion showing the different menus

- **Simcenter NX Motion**

This module allows the mechanism motion analysis to obtain displacements, loads, positions, interference or motion ranges, among many others. In order to create a successful kinematic simulation, first the components are defined as motion bodies, joints and the movement is created by adding drivers. Finally, the control can be achieved in several ways. **Figure 2.8** shows the crane in a motion analysis.



Figure 2.9: NX Motion showing an animation

- **NX Animation**

The animation is the output for the NX Motion, and it allows the generation of plots and data spreadsheets. An example of the animation can be seen in **Figure 2.9** In addition, it can generate motion envelopes and measure positions at any step moment.

## 2.3 Structural Analysis by the Finite Element Method

Structural analysis is a branch of engineering that applies a set of mechanical theories and physical laws with the intention of studying and predicting the behaviour of structures.[25]. A structure can be a bridge, building or a crane, and is defined as a group of links connected by joints in a particular configuration and withstanding loads.

A joint restricts the degrees of freedom of a part, depending on the type. Every rigid body has 6 degrees of freedom, as displayed in **Figure 2.10** and are defined as following:

1. Translation along X-axis
2. Translation along Y-axis
3. Translation along Z-axis
4. Rotation around X-axis
5. Rotation around Y-axis
6. Rotation around Z-axis

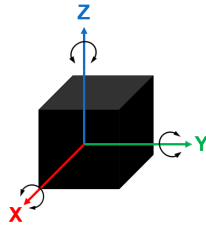


**Figure 2.10:** Degrees of freedom of a rigid body in space

There are several types of joints that restrict the movement of the links and define the load transfer. The two joints that will be used in this project are displayed in **Figure 2.11** and described as:

- **Revolute**  
Allows the rotation only in the X axis. The rest of the degrees of freedom are fixed. This constraint or joint is also known as "pin" or "hinge". This joint is used in the crane to move the three angular displacements.
- **Slider**  
Allows the translation only along the X axis. The rest of the degrees of freedom are fixed. This joint will be applied in the crane for all the telescopic parts.

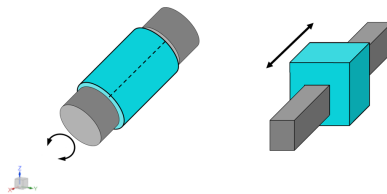


**Figure 2.11:** Revolute and slider joints

To perform an accurate analysis, it is necessary to determine the geometry of the part to test, the structural loads, boundary conditions and materials used. The results will contain support reactions, displacements and stresses.

Structural Analysis is often divided in three stages[26]:

- Establishing the boundary conditions and design loads
- Defining acceptance criteria
- Running the analysis

There are many applications of the finite element method such as acoustic simulations, fluid dynamics, thermal analysis and it is particularly applied to the structural analysis due to its capacities for calculating displacements and strains under a set of loads.[27]

### 2.3.1 Finite Element Method

The Finite Element Method (FEM) is defined as a numerical technique for solving partial differential or integral equations to obtain the evolution in time of the variables that represent the behaviour of a physical system and it is applied by dividing a rigid body into smaller, finite elements. Since the geometry of the studied structure has to be simplified and divided into smaller parts, FEM offers an approximation to the real exact solution. [27]

There are three main error sources that contribute to the complete FEM approximation model, and those are [27]:

- **Discretization error:** Represents the error created by the mesh finite element and size. It can be reduced by using a finer mesh, an element with more nodes or refinement zones. A mesh convergence study will directly impact and reduce this error.
- **Modeling error:** Represents the error caused by an incorrect model simplification and it can be fixed by increasing the accuracy of the model and assumptions. The evaluation of the original crane parts and an idealized model will provide an idea of the accuracy of the models.
- **Numerical error:** This error is caused by the use of computers to solve the equations and is usually very small.

#### Finite Elements

A finite element is a fraction or portion of the complete element or body. [27] There are many different types of finite elements, varying from 1D, 2D and 3D elements. A node is a joint point, and the most simple 1D element consists of two connected nodes. As the number of nodes increase, the computational effort and accuracy of the results increase. The finite element types are described as a shape followed by the number of nodes, and the list is displayed in **Table 2.1**. A mesh is defined as the complete set of elements that discretize a 3D model. It can consist of a single element type, or a combination.










Element Type	Element Name	Number of Nodes	Example
1D	1D Mesh	$\geq 2$	
2D	TRI3	3	
	TRI6	6	
	QUAD4	4	
	QUAD8	8	
3D	TET4	4	
	TET10	10	
	HEX8	8	
	HEX20	20	

Table 2.1: Finite Element Types

The squared or rectangular elements such as *QUAD* and *HEX* are most used for defined simple shapes, while the triangular elements such as *TRI* and *TET* are used for more irregular shapes. Therefore, for the FEA study case, the focus will be in the triangular elements and an approximation using 1D Beam elements will be developed. [28]

## 2.4 Maintenance and Monitoring

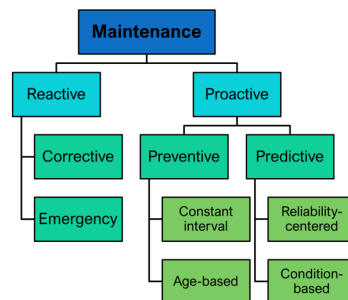


Figure 2.12: Different maintenance approaches [5]

The term maintenance refers to a process of necessary actions with the purpose of restoring or preserving an item or equipment within a set of operating conditions.[5] There are several approaches to maintenance, displayed in **Figure 2.12**. The two main classi-

fications: reactive and proactive, define the moment when the maintenance takes place. Reactive maintenance refers to all unplanned services provided after a failure or defect has occurred, while proactive maintenance refers to all planned services provided to an equipment without any failures or problems.

Reactive maintenance is sub-divided into corrective and emergency maintenance. The objective of corrective maintenance is to fix an issue that has already occurred, to restore the equipment back to operation. Emergency maintenance is an urgent service that is applied to avoid permanent consequences. The cost of reactive maintenance is high mostly because the equipment has already been damaged, usually requiring spare parts, and the repairing process becomes an urgent task to reduce the operational downtime.

Proactive maintenance is divided into two sub-groups, which are preventive maintenance and predictive maintenance.

### **2.4.1 Preventive Maintenance**

Preventive maintenance is a set of planned services at specific intervals, reducing the probability of failure. [5] These intervals are calculated considering the product lifetime and probability failure rates. This type of maintenance, is sub-divided into two groups:

- 1. Constant interval**

For this type of maintenance, the intervals are done at a constant interval pace, which is calculated using probabilities of failure.

- 2. Age-based interval**

This type of interval sets maintenance check-points according to the operational amount of hours of a product.

The cost for preventive maintenance is reduced in contrast with reactive maintenance, and since this strategy relies in probabilities and estimates, occasionally requires reactive maintenance. The downside of this strategy is the amount of maintenance occurrences.

### **2.4.2 Predictive Maintenance**

Predictive maintenance applies a set of methods to predict when the product requires maintenance. The methods vary among a set of product status revisions, to the monitoring through the application of technology and sensors. Predictive maintenance was created with the purpose of reducing the total costs in Maintenance, as shown in **Figure 2.13**.

The two components of the total cost are prevention costs, and repair costs. Since preventive maintenance provides a larger amount of services with smaller repair cost, the total cost is still high. On the other hand, reactive maintenance has a smaller number of

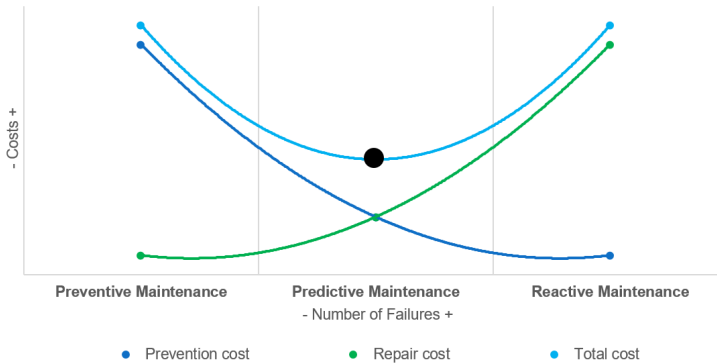


**Figure 2.13:** Maintenance costs plot [5]

prevention costs but each of them has a high repair cost. Therefore, the goal of predictive maintenance is to reduce the prevention and repair cost by delivering the service right when it is required. Predictive maintenance is divided into two sub-groups:

### 1. Condition-based maintenance

The time-span for this type of maintenance is defined by the condition of the product or component which is monitored constantly. The variable that is monitored needs to accurately reflect the product status. [5] This system provides advantages such as an increased failure prediction rate and supports the identification of the failing components. The main disadvantage is the cost and installation of sensors and monitoring systems.

### 2. Reliability-centered maintenance

This method for maintenance uses reliability data to define a cost-efficient maintenance schedule. For this study, the failure modes are analyzed using a well-known *Failure Modes and Effects Analysis* engineering study.

The new trends in maintenance are being described as *Health Monitoring* since they involve deep system analysis, statistical modeling and technology systems to keep the product working in an optimal range.

## 2.5 Structural Analysis & Maintenance-Monitoring

### 2.5.1 Structural Health Monitoring

A topic that is often mentioned related to structural analysis and predictive maintenance is Structural Health Monitoring (SHM), which is a method of applying sensors to structures in order to monitor the conditions of the structures. *"It has been widely applied in various*



*engineering sectors due to its ability to respond to adverse structural changes, improving structural reliability and lifecycle management.”[29] It is mostly applied in the aerospace, energy and civil engineering areas.*

Structural Health Monitoring of structures impacts the safety, inspection, maintenance and repair processes of structures. [6] The biggest challenges for SHM systems design are:

- The structure is located in a hostile environment - salt, water and complete exposure to the weather.
- The instrumentation applications for corrosive and hostile environment become more restricted.
- Load uncertainties due to the environment.

Among the benefits obtained when applying Structural Health Monitoring, are:

- Extension of structure lifespan
- Reduced inspection costs
- Minimized predictive maintenance
- Data gathering for usage monitoring
- Damage detection
- Fatigue Life predictions

### 2.5.2 Maritime Structures and Ship Monitoring Systems

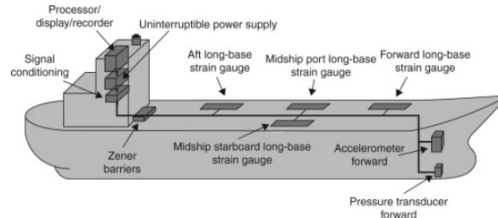


**Figure 2.14:** Typical Hull Monitoring System for a Bulk Carrier [6]

The techniques for Structural Health Monitoring used in ship and offshore structures have a different classification. For the ships, they are called Hull Monitoring Systems (HMS) and contain sensors in common locations to measure specific parameters, as shown in **Figure 2.14**. [6] For the maritime structures, it is called Structural Integrity Assessment and it is performed to extend the life of the facilities or structures. This is related to the project since the crane belongs to the maritime industry and is mounted in a ship.

A hull monitoring system "enables the operator of the vessel to monitor all relevant responses, such as motions, accelerations, loads, bending moments, stresses, etc.[6]", providing real-time information for support and rational guidance to prevent measures in heavy conditions. [30]

For these cases, it is of high importance to monitor the fatigue, cyclic forces and strains in the structural elements, to determine the effect of the strength and stiffness degradation in structures. The gauge type used for these purposes is a fatigue gauge, and they are located in stress-concentrated areas for the purpose of detecting the fatigue cracks.[6]

### 2.5.3 Bridge Monitoring Systems

In Japan, Structural Monitoring is applied to bridges, buildings and roadways. The technique applied is monitoring through vibration. They have been developing the techniques by gathering the data, and obtaining inputs for the "redevelopment of designs of new constructions"[7] Over the time, they get a vast data set accumulated to understand the behavior of the structure under different load conditions.

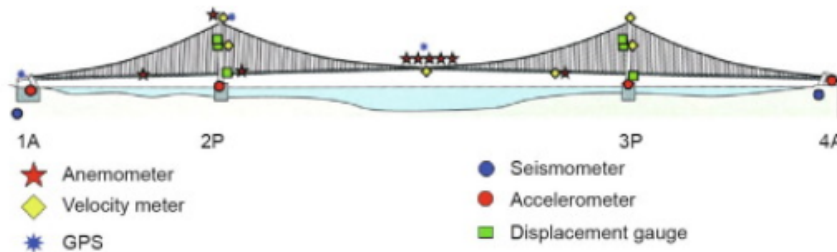


**Figure 2.15:** Structural Monitoring of the Akashi Kaikyo bridge [7]

As an example case, **Figure 2.15** shows the structural monitoring and several sensors mounted in a bridge. 1A & 4A are the anchorages, while 2P & 3P are the main pylons.[7] It is important to understand what types of sensors the structural monitoring relies on, in order to understand the outputs. In this case, the bridge used the following sensor types:

- **Anemometer**  
Device for measuring the speed of airflow in the atmosphere. The ranges are from 5 to 100 knots. [31]
- **Seismometer**  
Highly sensitive instrument that detects movements in the earth's surface.[32]
- **Accelerometer**  
This sensor measures the acceleration in two or three axis-vector components. [33]

- **Displacement gauge**

Measures the displacement range between the current position of an object and its reference. [34]

For this project, a set of strain gauges will be used for the structural monitoring of the maritime crane. A strain gauge measures the applied forces, pressures, stresses and strains. It is an essential sensor for the mechanical measurement of structures. [35] The suggested positions where they can be installed will be discussed according to the results of the structural simulations.

## 2.6 Digital Twin & Structural Analysis

There are combinations applying digital twins developed exclusively for structural analysis. Since the very beginning, digital twins were developed to track structural changes by the NASA. [11]

A bending test beam digital twin was developed on [13] to demonstrate the concept and capabilities. This test was chosen due to its low complexity. The test was run and the FEM simulation was triggered every time new data was detected. They developed a dashboard where the real data versus the digital twin data was compared. The FEM simulation was able to run using as inputs the real force applied or the displacement values. The test was successful, and the data had a deviation within the error margins. It is mentioned that there are many factors that can contribute to these error margins: the manufacturing tolerances, the material properties, the force angle, etc.



# Methodology

## 3.1 Study Case

The starting point for this master thesis was a 3D surface model of the Palfinger crane, model PK-65002-M in the software Siemens NX 1892, shown in **Figure 3.1**. It was developed by professor Terje Rølvåg from NTNU. The 3D model was originally assembled using the coordinates as reference points, so it contained no constraints.

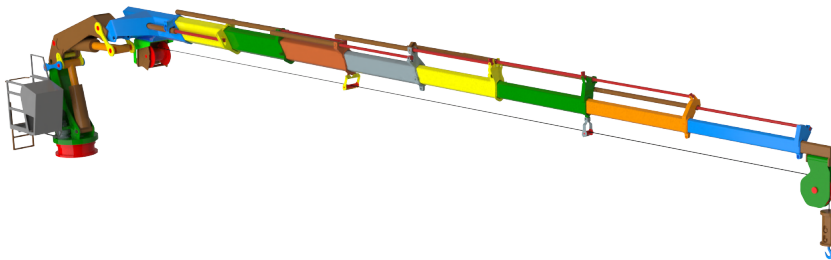


**Figure 3.1:** Initial 3D model of the Palfinger crane

The model consists on 43 parts as enlisted in **Table 3.1**. The parts were separated in two groups: structural, which are the parts that were selected for the finite element analysis, and the functional, which were added together with the structural into the kinematic model. **Figure 3.2** displays the crane model, with the structural parts numbered and highlighted in blue, while the functional parts are shown in grey.

Part Type	Number	Name
Structural	1	Yaw bearing support
	2	Yaw support
	3-4	Pitch link 1 and 2
	5-12	Tele 1 to Tele 8
	13	Tele end
Functional	14	Winch
	15	Winch pulley
	16-17	Wire guide 1 and 2
	18	Wire
	19	Basket
	20-27	Cylinder 1 to 8
	28-35	Piston 1 to 8
	36-37	Tilt cylinder 1 and 2
	38-39	Tilt piston 1 and 2
	40-41	Double link 1 and 2
	42	Hinge bracket
	43	Load cell hook

**Table 3.1:** Bill of materials of the initial 3D model

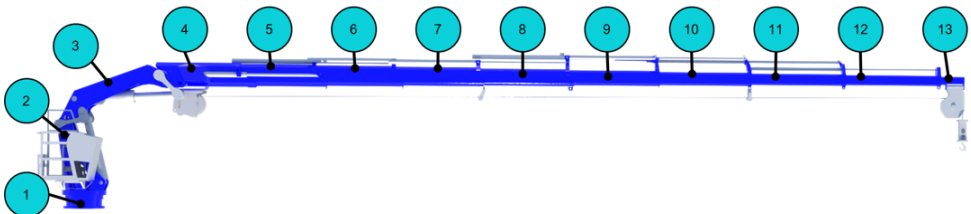


**Figure 3.2:** 3D model of the Palfinger crane highlighting structural components

### 3.1.1 Assumptions

The crane model that will be studied in this case is a Palfinger PK-65002-M, which according to the supplier is a foldable knuckle boom crane, and the specifications are shown in **Table 3.2**.

Since the crane is mounted in the NTNU Gunnerus ship, it is important to mention that for both the structural and kinematic simulations the ship dynamics will not be considered. The crane will be constrained as fixed in the ground.

Parameter	Value
Maximum lifting capacity	22,000 kg
Dead weight	4,555 kg
Maximum hydraulic outreach	20.5 m

**Table 3.2:** Palfinger PK-65002-M operational specifications [1]

For the structural analyses it is assumed that while the crane is within the operational ranges specified in the product data-sheet, the hydraulic cylinders are strong enough to maintain the crane in a defined position. Therefore, the hydraulic cylinders 3D models are initially not considered in the finite element analyses, but they are modeled as a beam part and tested in contrast to a model without. In addition, the loads applied in both kinematic and FEA analyses are according to the data from **Table 3.3**

Hydraulic outreach [m]	Maximum lifting capacity [kg]
Maximum	22,000
4.4	13,460
5.8	10,250
7.5	7,940
9.4	6,180
11.4	4,830
13.7	3,780
15.8	3,030
18.4	2,440
20.4	1,970

**Table 3.3:** Palfinger PK-65002-M detailed lifting capacity [1]

### 3.1.2 Limitations

The digital twin for the maritime crane will be explored in this project with the purpose of understanding the development phases and its potential applications. The connection between the virtual and physical models will not be established in this study, but either it will be simulated with data, and the necessary inputs and outputs for connecting the two counterparts will be established and documented. This simulation will allow the project to be a proof of concept for the digital twin technology.

The accuracy of the whole digital twin depends directly on the accuracy of the 3D surface model. As an initial test, the dead weight of the crane 3D model was compared according to the product specifications, and the results can be found in **Table 3.4**. This means that only due to the variations between the product specification and the model, the accuracy is compromised by at least a 10 %. Since the objective of this project is to develop a virtual

twin and to map the requirements for upgrading it to a digital twin, the accuracy is not an issue because the 3D model can be easily updated at any time in the next stages of the project; but it is important to mention that this limitation exists.

Test	Weight [kg]	Accuracy [%]
Product specification	4,555	100
3D model calculation	4,121	90.5

**Table 3.4:** Crane dead weight comparison test

The physical sensors required to be mounted in the physical crane structure are expensive, therefore, several iterations of the structural simulations will be done to find the most important locations and use the minimum amount.

### 3.2 Research Method

The digital twin of the maritime crane will be developed using Siemens NX 1892 applying a simulation-based design approach, where two separate models will be created using different NX applications, and are shown in **Figure 3.3**. The structural and the kinematic simulation will feed the digital twin and each of them has particular milestones to complete the objective. As stated previously, simulation-based design will be applied for each test, and it consists on a cycle of three iterative steps: design, simulation and verification.

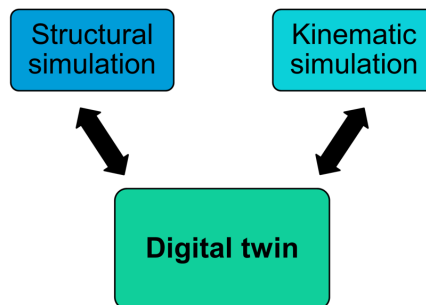


**Figure 3.3:** Simulation models

### 3.3 Main model preparation

Initially, both models share the first three steps, which purpose is to understand the degrees of freedom of the crane, create an assembly with the proper constraints, and program the



NX Expressions to control the joints of the crane. This will allow us to define the initial position of the crane without changing the constraints or moving part by part. The first steps for preparing the model using NX Modeling are defined as following:

### 1. Studying the crane:

The objective of this study is to map how the crane moves, determine limits for the degrees of freedom and identify possible challenges to develop the digital twin. The crane has two types of joints, which were explained previously, in chapter 2. It has three revolute joints, and nine slider joints, as displayed in **Figure 3.4**

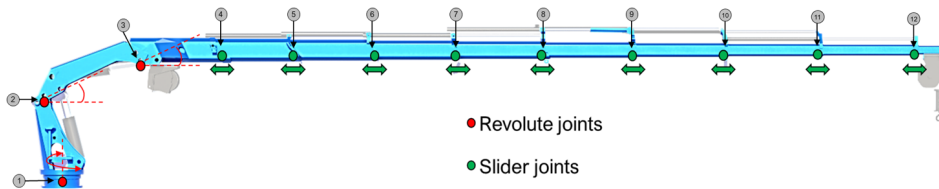


**Figure 3.4:** Crane joints

For every joint, there will be one expression that allows to control the positions. The variable or expression names and the programmed limits according to the product specifications and mechanism study is shown in **Table 3.5**. The joint number is referenced according to **Figure 3.4**.

Joint Type	Joint number	Expression Name	Programmed limits
Revolute	1	<i>BaseAngle</i>	No limit
	2	<i>RevAngle1</i>	-40° to 40°
	3	<i>RevAngle2</i>	-25° to 25°
Slider	4	<i>DistTele1</i>	30 to 1676 mm
	5	<i>DistTele2</i>	30 to 1829 mm
	6	<i>DistTele3</i>	30 to 1931 mm
	7	<i>DistTele4</i>	30 to 2030 mm
	8	<i>DistTele5</i>	150 to 2152 mm
	9	<i>DistTele6</i>	120 to 2203 mm
	10	<i>DistTele7</i>	120 to 2258 mm
	11	<i>DistTele8</i>	120 to 2265 mm
	12	<i>DistTeleEnd</i>	450 to 554 mm

**Table 3.5:** List of joints with the expression name and limits as used in NX

A possible challenge was observed due to the crane geometry and it is located in the sliding or telescopic parts of the crane. The parts do not make contact with each other, and there is a gap between 5 to 15 mm per face. A transversal cut across the length of the parts was made to visualize this gap, and it is shown in **Figure 3.5**. This gap might represent that there is an additional material that makes contact, but

it is not mentioned in the crane specifications. It will be a challenge for the structural analysis.

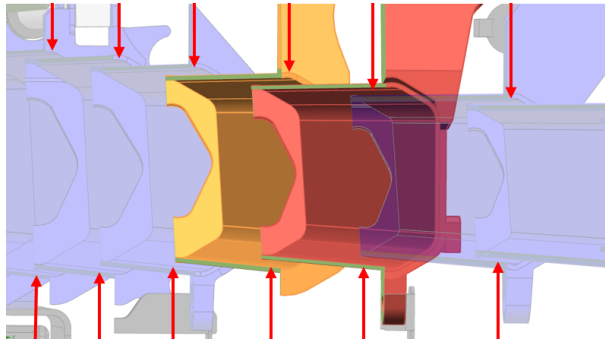


**Figure 3.5:** Gap between the telescopic parts

## 2. Creating the assembly constraints:

In this step, the data gathered from the crane study will be translated into assembly constraints. Due to the crane complexity, most of the constraints used for developing the assembly were *center*, *hinge* or *revolute*, and *slider*. The limits were selected as displayed in **Figure 3.6**.

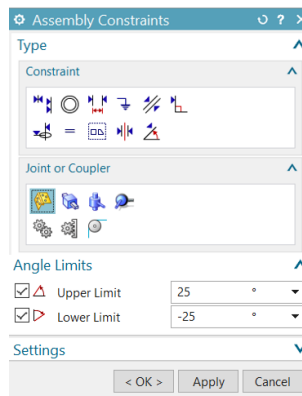


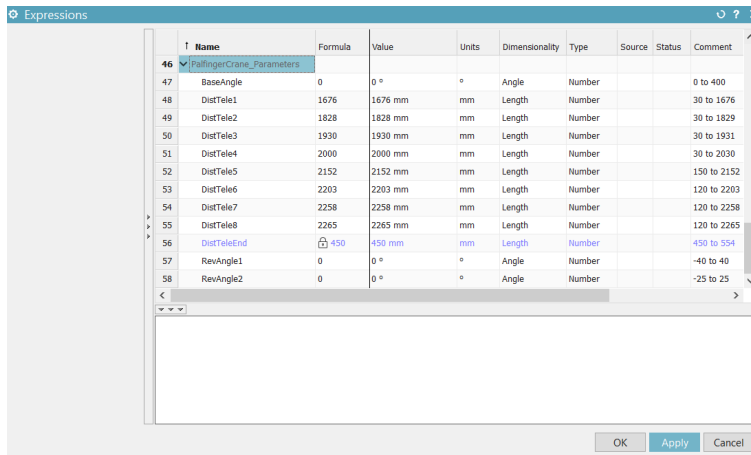
**Figure 3.6:** Defining the joint limits for a Hinge or Revolute joint in NX for *RevAngle2*

After defining the constraints for every part, using the NX Modeling tool *move*, it was possible to slide and rotate the parts using the limits, in order to validate that the constraints were assigned properly.

## 3. Programming the expressions:

For this step, a variable for every joint was defined, and it controls the position of the

crane. This tool will be useful to define the initial position of both the structural and kinematic simulations. The NX Expressions list is displayed in **Figure 3.7**, and it includes the values, units, and a comment defining the limits. An additional benefit of using this tool is that the parameters can be changed simultaneously in the same window, without having to change constraint by constraint, and if the values used as input are out of the limits, they are ignored.



#	Name	Formula	Value	Units	Dimensionality	Type	Source	Status	Comment
46	FallingCrane_Parameters								
47	BaseAngle	0	0 °	°	Angle	Number			0 to 400
48	DistTele1	1676	1676 mm	mm	Length	Number			30 to 1676
49	DistTele2	1828	1828 mm	mm	Length	Number			30 to 1829
50	DistTele3	1930	1930 mm	mm	Length	Number			30 to 1931
51	DistTele4	2000	2000 mm	mm	Length	Number			30 to 2030
52	DistTele5	2152	2152 mm	mm	Length	Number			150 to 2152
53	DistTele6	2203	2203 mm	mm	Length	Number			120 to 2203
54	DistTele7	2258	2258 mm	mm	Length	Number			120 to 2258
55	DistTele8	2265	2265 mm	mm	Length	Number			120 to 2265
56	DistTeleEnd	450	450 mm	mm	Length	Number			450 to 554
57	RevAngle1	0	0 °	°	Angle	Number			-40 to 40
58	RevAngle2	0	0 °	°	Angle	Number			-25 to 25

**Figure 3.7:** List of expressions programmed in NX

After this main model preparation, the crane can be set in any position within the allowed limits, and be used as the initial point for both the structural and kinematic simulations. From this point on, the model splits into the two final models: structural and kinematic, both with their own milestones and challenges.



# Structural Simulation

In this section, the methodology followed for developing the structural simulation by the FEM using NX will be detailed, starting with the set of validation tests, followed by the setup of the different models developed and tested. It is important to explain that for every test, the simulation-based design methodology will be applied. The particular NX module used for every step is shown in **Figure 4.1**.

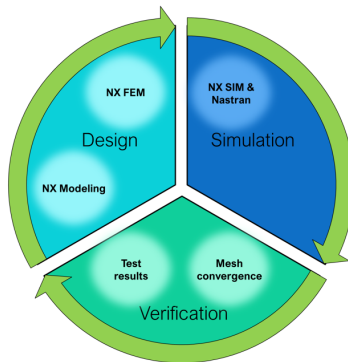


**Figure 4.1:** Simulation-based design diagram for the structural simulation

For the design stage, NX Modeling and NX FEM will be used to edit the parts and create the mesh for the 3D models. For the simulation stage, NX Sim will be used to define the boundary conditions and Nastran to solve the model. For the verification stage, a mesh convergence test and the test results will be documented in order to find possible improvements for the next SBD iteration.

As displayed in **Figure 4.2**, the test progression will be made building up the final model, part by part, with a set of defined checkpoints. Initially, the slider and revolute joints will be tested individually and then assembled, to complete the partial and complete tests.

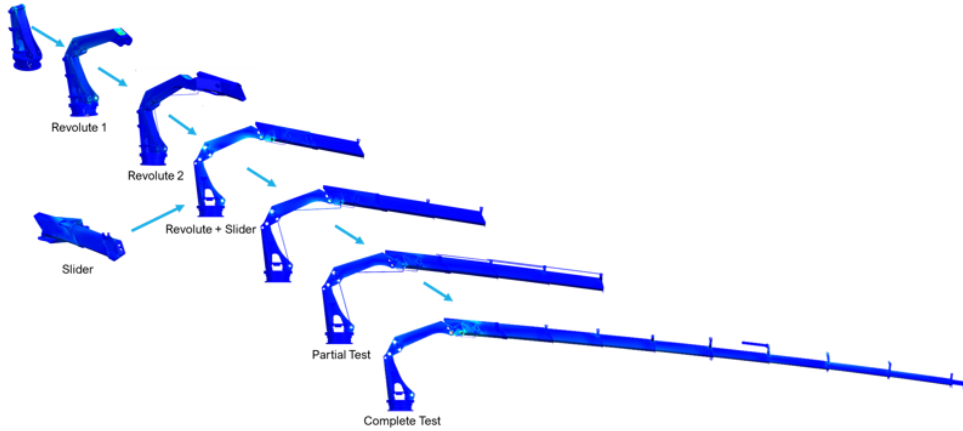


Figure 4.2: Progression of the tests

## 4.1 Model selection and considerations

The initial step is to define the model to use. The complete original crane model contained 43 parts, and the selected model for the structural analysis is displayed in **Figure 4.3**, and has 13 parts. The degrees of freedom are also displayed in the figure, counting 2 revolute joints and 9 slider joints. For this analysis, the base angle degree of freedom was neglected.

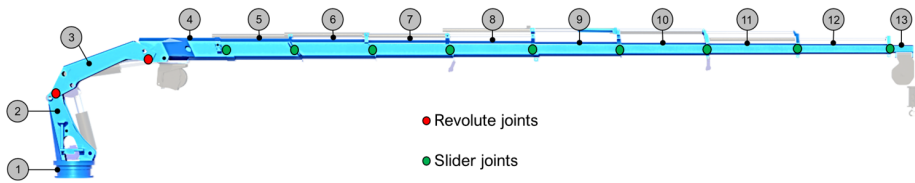
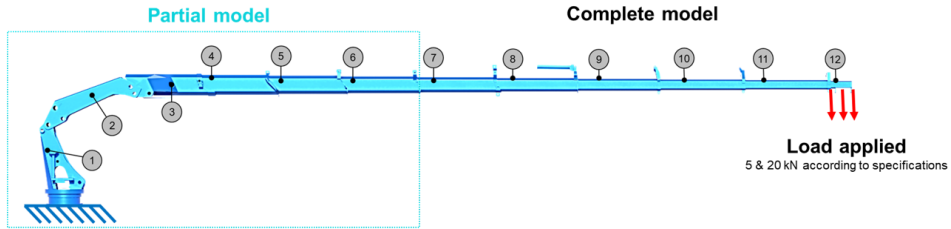


Figure 4.3: Degrees of freedom for the structural analysis simulation

Since the tests were made by building up part by part, the two main configurations used to test the simulations are displayed in **Figure 4.4**. The partial model is a validation of the crane behavior with the joint combinations before assembling the complete model. It includes the first 6 parts, testing two revolute joints and three slider joints. After this model was validated, the complete model was assembled and tested, adding part by part. In addition to these configurations, the revolute test includes parts from 1 to 3, and the slider joint includes only parts 3 and 4.



**Figure 4.4:** Partial and complete models, showing the boundary conditions

As displayed in **Figure 4.4**, the boundary conditions are specified for the tests as the base being fixed in the ground, and a load applied at the ending part. Two different loads were used: 5 kN, to validate the crane model, and 20 kN, to test the maximum lifting capacity at the maximum hydraulic outreach of 20.4 meters.

## 4.2 Mesh convergence study

The first test for the FEM model development is a mesh convergence study, which is a method for validating the element type and size within a finite element method model.

The purpose of this test is to define a balanced mesh size regarding accuracy and simulation time that will be used throughout all the simulations. This study was done using the individual parts of the crane for the structural analysis. This means that there are 13 parts that were studied and compared according to the simulation time, displacement and stress values. Each part was meshed individually, then set the boundary conditions as fixed in one end, and a force applied in the other end.

The mesh convergence test for the first 6 components of the crane is displayed in **Table 4.1**, where the element type selection was based not exclusively in the simulation time, but considering the most accurate result. This means that the simulation with the smallest element size using *CTetra(10)* elements was considered as the reference. As observed in the table, the values for displacement converge when using the element type *CTetra(10)*, while the values for *Ctetra(4)* show a variation between 5% to 30%.

For the stress results, there is a general variation that increased when using the *Ctetra(4)* elements. As stated previously, *CTetra(4)* has 4 nodes while *Ctetra(10)* has 10 nodes, therefore the simulations using the 4-noded-element are considerably faster, reducing the simulation time by a 60% to 85%. The elements that were used for the simulations are marked in the last column with a star symbol. It is important to mention that the crane part 6 had difficulties in the meshing process.

The mesh convergence test for the components 7 to 13 of the crane is displayed in **Table**

Part	Element Type	Element size	Displacement [mm]	Stress [MPa]	Simulation time [s]	
1	CTetra(10)	20	0.0070	8.001	43	
		50	0.0069	7.303	13	*
		53.5 (auto)	0.0069	6.808	17	
1	CTetra(4)	20	0.0065	6.107	23	
		53.5 (auto)	0.0058	4.341	2	
		30	1.440	250.55	330	
2	CTetra(10)	40	1.441	234.77	199	
		46.2 (auto)	1.437	244.19	171	*
		40	1.295	168.36	25	
2	CTetra(4)	46.2 (auto)	1.241	152.25	16	
		10	0.515	30.19	300	
		30	0.514	26.17	55	
3	CTetra(10)	46.4 (auto)	0.514	20.89	30	*
		10	0.510	17.27	120	
		46.4 (auto)	0.486	15.56	11	
4	CTetra(10)	15	0.338	52.06	261	
		30	0.335	51.58	111	
		33.5 (auto)	0.334	43.89	87	*
4	CTetra(4)	10	0.267	22.61	95	
		33.5 (auto)	0.227	25.24	35	
		10	0.538	35.06	340	
5	CTetra(10)	28.8 (auto)	0.537	41.43	57	
		60	0.535	34.96	29	*
		10	0.532	25.85	124	
5	CTetra(4)	28.8 (auto)	0.525	19.12	19	
		27.9 (auto)	0.666	41.60	59	*
		27.9 (auto)	0.657	24.26	22	

**Table 4.1:** Mesh Convergence Analysis for the structural parts 1-6

**4.2**, where the element type selection followed the same strategy than the first set of components. The difference in this table is the element size selection, where the auto value was a middle point for the *Ctetra(10)* element type. As observed in the table, the displacement results have a very small variation of 0-2% with a considerable impact in reducing the simulation time by an average of 90%. In contrast, the biggest variation is noted in the stress results. Therefore, in most of the cases, the auto value was used.

As an example of the mesh convergence test, **Figure 4.5** shows the visual mesh variation for two element sizes for the *Ctetra(10)* element type. **Figure 4.5a** has a 10 mm element size, with displacement results of 0.515 mm, while **Figure 4.5b** has a 46.4 mm automatic element size with displacement results of 0.514 mm. The main difference between these two iterations is the simulation time, which gets reduced by 90% or 270 seconds, by using a bigger element size.



Part	Element Type	Element size	Displacement [mm]	Stress [MPa]	Simulation time [s]	
7	CTetra(10)	10	0.603	30.53	250	
		29.9 (auto)	0.602	32.17	45	
	CTetra(4)	50	0.601	30.52	30	*
		10	0.600	23.46	106	
8	CTetra(10)	29.9 (auto)	0.596	17.72	17	
		15	1.206	61.26	140	
	CTetra(4)	25 (auto)	1.204	74.36	67	*
		50	1.201	46.54	34	
9	CTetra(10)	10	1.180	38.71	83	
		25 (auto)	1.178	34.21	40	
	CTetra(4)	27.2 (auto)	1.582	61.37	64	*
		45	1.580	71.35	35	
10	CTetra(10)	27.2 (auto)	1.575	35.62	28	
		45	1.553	38.04	14	
	CTetra(4)	10	3.329	84.83	300	
		25.7 (auto)	3.285	80.52	49	*
11	CTetra(10)	60	3.256	120.88	22	
		10	3.307	67.48	77	
	CTetra(4)	25.7 (auto)	3.319	66.68	17	
		10	4.416	121.12	196	
12	CTetra(10)	30.5 (auto)	4.415	108.43	33	*
		60	4.414	90.4	16	
	CTetra(4)	10	4.222	92.63	77	
		30.5 (auto)	4.380	81.08	14	
13	CTetra(10)	10	6.942	159.71	180	
		29.3 (auto)	6.941	133.01	33	*
	CTetra(4)	60	6.938	112.32	14	
		10	6.944	120.74	72	
13	CTetra(10)	29.3 (auto)	6.889	97.9	12	
		10	1.472	88.64	65	
	CTetra(4)	40.2 (auto)	1.468	75.06	10	*
		80	1.462	66.74	5	
CTetra(4)	10	1.475	65.84	28		
	40.2 (auto)	1.417	63.15	4		

**Table 4.2:** Mesh Convergence Analysis for the structural parts 7-13

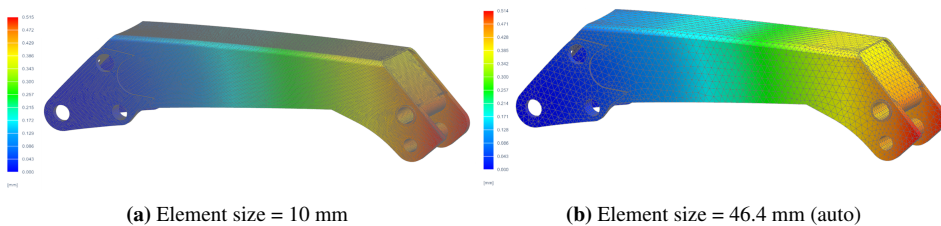


**Figure 4.5:** Mesh size comparison for part 3 using *CTetra(10)*, displaying displacement results

## 4.3 Validation tests

In order to develop the model for the structural analysis applying the finite element method, a set of validation tests were necessary to define the best practices for the final models. As shown in **Figure 4.6**, four main types of tests were realized. The first and second tests are for the revolute and slider joints, with the purpose of finding the most accurate representations of the degrees of freedom of the two pins in the crane structure and the 10 telescopic parts. The third test is a verification of the crane model tested with and without the hydraulic cylinders in the structure. Finally, the geometry idealization is a comparison between the original parts and a simplified model in order to reduce computational time. A table with the results summary will be displayed at the end of every section.

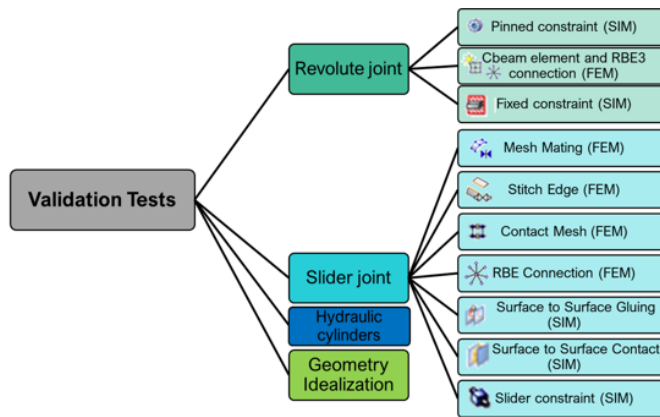


**Figure 4.6:** Validation tests for the structural simulation

### 4.3.1 Revolute joint

The maritime crane has three revolute joints as explained previously, and only two of them are considered for this structural simulation. There are several ways of simulating this type of degree of freedom in NX. For this test, three different methods were studied and tested, in order to find the most accurate and efficient revolute joint constraint.

#### 1. Pinned constraint

This constraint can be found in the NX Sim module, and fixes all degrees of freedom, except the rotating direction. There is no option to constrain that rotation, therefore when simulating, the result presents a large displacement. **Figure 4.7** displays both the test setup and the results. In **Figure 4.7a**, the two revolute joints are displayed with the pinned constraint and a load applied at the end.

In **Figure 4.7b** the results for displacement of the test are shown, obtaining very high values due to the pinned constraints being able to move freely. In addition, the

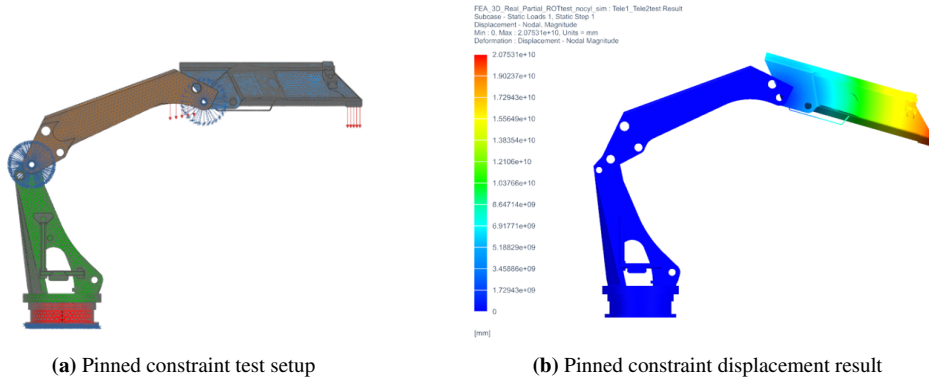


**Figure 4.7:** Pinned constraint for the revolute joint test

part 3 does not show any displacement.

## 2. C-beam and RBE3 connector

For this test, a beam *superelement* was created for each joint, and connected to the mesh in the NX FEM module. A superelement is a simplified version of an element which can simulate assembly constraints while maintaining low the simulation time.[24] In addition, the superelement can be defined as a beam with a specified cross-section and material which in this case was steel.

In **Figure 4.8**, the test setup and the results are displayed. The revolute joints contain a green color as part of the mesh in **Figure 4.8a**, and in **Figure 4.8b**, the displacement result shows an uniform displacement from the part 3 to the part 4.

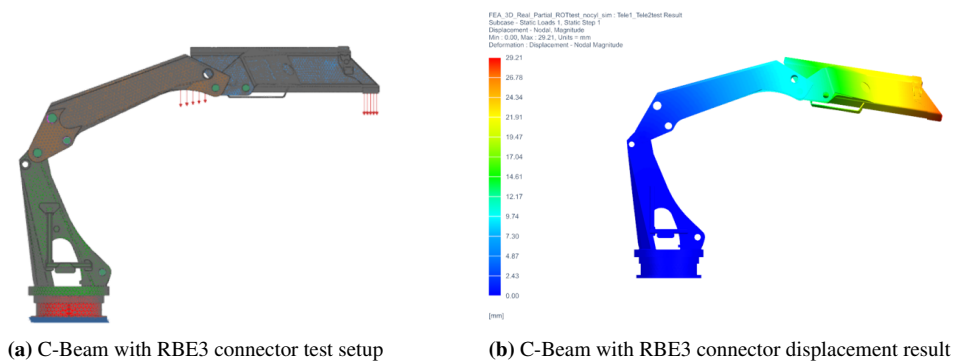


**Figure 4.8:** C-Beam with RBE3 connector for the revolute joint test

### 3. Fixed constraint

The last test for the revolute joint consists in applying a fixed constraint to the rotation axis for both joints in the NX Sim module. In **Figure 4.9**, the test setup and the results are displayed. The fixed joints show a blue color as part of the visualization in the test setup displayed in **Figure 4.9a**, and **Figure 4.9b** shows the displacement result, where again the displacement appears only in the last part.

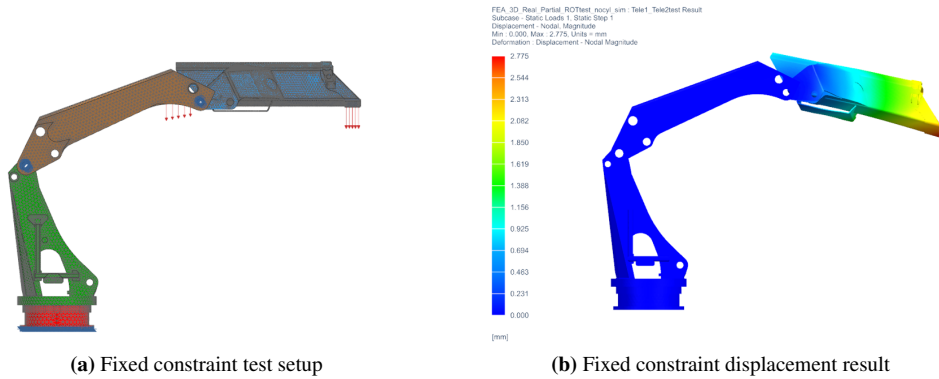


**Figure 4.9:** Fixed constraint for the revolute joint test

### Revolute test results

A summary of the results is displayed in **Table 4.3**. As conclusion of the revolute test, the pinned constraint is not an accurate method to model the revolute since it allows free rotation in the joint axis. The fixed constraint is not accurate, since it restricts completely the movement, only showing displacement in the last part of the crane.

The C-beam and RBE3 connection represent the most accurate method to simulate the revolute joints, since it allows an uniform displacement, in addition to having a low simulation time in comparison with the other results. The star in the table shows the method that was selected.

Test number	Revolute joint strategy	Simulation Time [s]	Displacement [mm]	
1	Pinned constraint	636	20751000000	
2	C-beam and RBE3	235	29.21	*
3	Fixed constraint	224	2.775	

**Table 4.3:** Results for revolute joint validation tests

### 4.3.2 Slider joint

The maritime crane has nine slider joints, which are the telescopic parts that allow the maximum extension up to 20.4 meters. As mentioned previously, the telescopic parts present a gap, and do not make contact with each other. This is a particularly challenging task to model in a FEM analysis. The slider joint method will be used 9 times across the model, so it is very important to define it properly. Therefore, 7 different methods were tested by using only the parts 4 and 5.

#### 1. Slider constraint

The first attempt was to apply a slider constraint in the NX Sim module. This test was not successful since the constraint allows the sliding across the movement axis, causing that the part moves freely and the simulation fails. There is no option to constraint the sliding range. Therefore this method was not successful.

#### 2. Mesh mating

The mesh mating function is in the NX Fem environment, and it connects two separate solid bodies by creating elements in between their meshes. This method is time consuming when updating the mesh with the added elements in between. In **Figure 4.10**, the mesh mating test setup and the result are displayed.

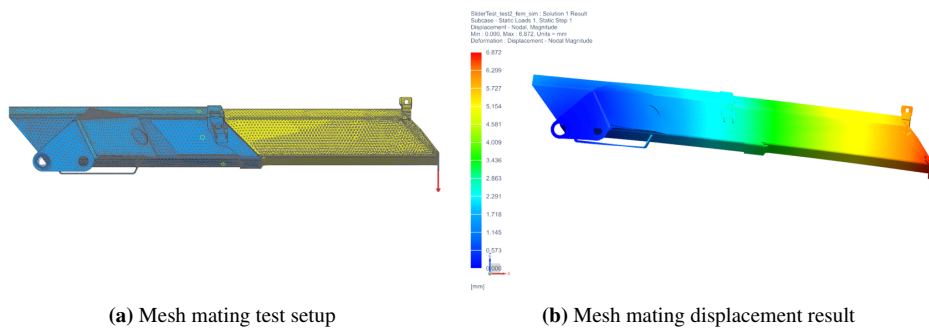


**Figure 4.10:** Mesh mating for the sliding joint test

In **Figure 4.10a**, the test setup is shown. To generate the mesh mating conditions, a set of matching faces or face pairs had to be selected. Therefore, the yellow dots represent the merging faces. Since the telescopic parts have a complex geometry, it was not possible to select all the faces, but the selection was made symmetric. In **Figure 4.10b**, the results show a regular displacement distribution.

In **Figure 4.11** the effect of using the mesh mating method is displayed. This method adds an irregular section of material, changing the shape of the parts. Since the aim of this project is to develop a digital twin, if the parts are modified, there would be an impact if compared with the physical parts.

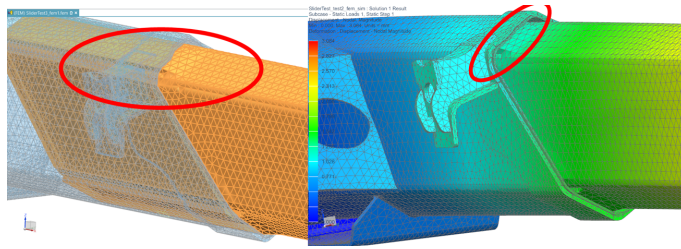
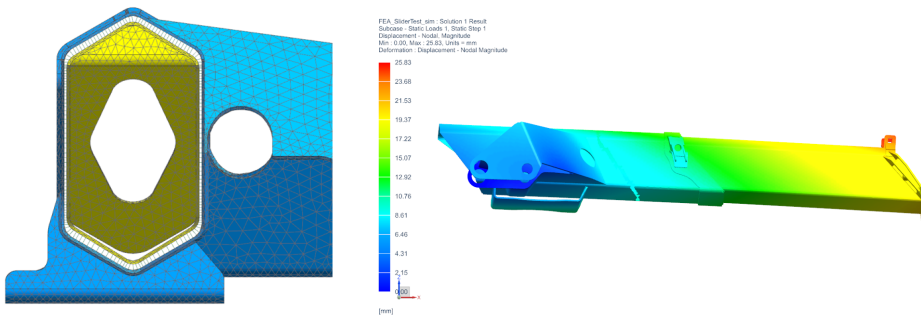


**Figure 4.11:** Mesh mating adding irregular material between the parts

### 3. RBE3 connection

The method applied is an RBE3 connection from an element edge to an element face in the NX FEM module. This means that only the ending edges of one of the telescopic parts were connected to the face of another part. **Figure 4.12** shows the RBE3 connection and the test results.



**(a)** RBE3 connection visualized in the gap between the telescopic parts

**(b)** RBE3 connection displacement result

**Figure 4.12:** RBE3 connection for the sliding joint test

The connection of the edge to the face using RBE3 elements is detailed in **Figure 4.12a**, and the displacement results are displayed in **Figure 4.12b**, where a cyan line shows where the connection took place.

### 4. Surface to surface gluing

This method of connecting the parts can be found in the NX Sim module and it joins two surfaces, creating a volume, or as named by the software, a *glue*, without any material specifications, located between the parts that can be plotted. It allows the transference of loads between the parts, and restricts the movement of the parts, which behave as if they were welded. **Figure 4.13** shows the test setup and the results.

The method of creating the union between the surfaces is to select two regions, and a search distance to find the other surface. **Figure 4.13a** shows the test setup and the visualization of the surface to surface gluing. The displacement results are displayed in **Figure 4.13b**, where the displacement is transferred in an uniform way.

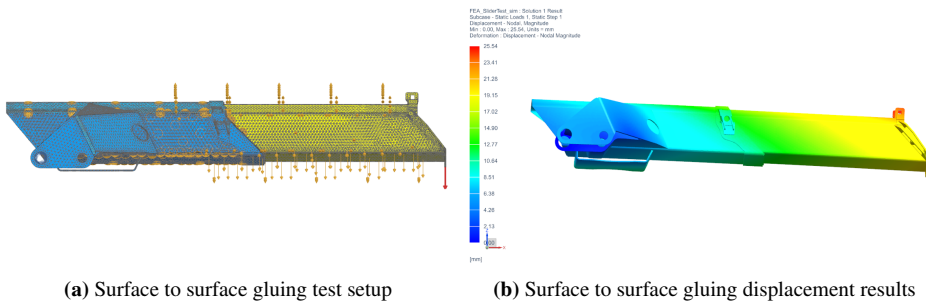


**Figure 4.13:** Surface to surface gluing method for the sliding joint test

The volume created between the parts can be visualized as shown in **Figure 4.14** which grants a clear image of how the forces are distributing in the gaps with the loads simulated. The crane parts were set up as mesh visualization to observe the glue or contact volume in the location between the parts.

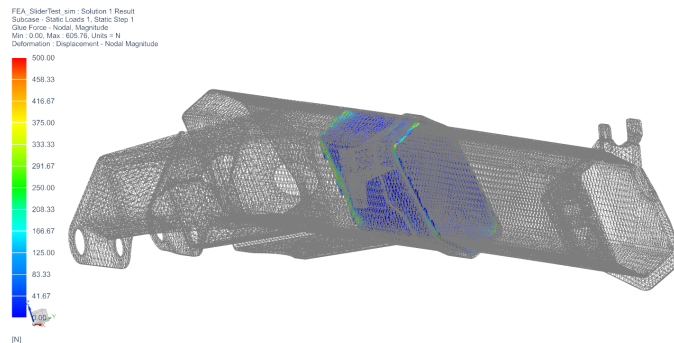


**Figure 4.14:** Surface to surface gluing: visualization of the material or *glue* force results

## 5. Surface to surface contact

This method of modeling contact is located in the NX Sim module and it allows sliding and free movement within the parts. The parameters were defined selecting contact regions, but the simulation lasted more than 6 hours without the contact solver converging, as shown in **Figure 4.15**. The conclusion is that since this contact allows the movement, the parts move and the simulation crashes. Due to the high

simulating time and the degrees of freedom, this method was not successful.

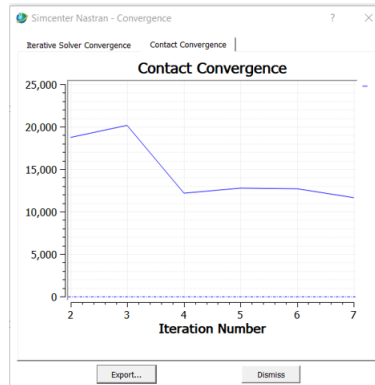


**Figure 4.15:** Unsuccessful contact convergence plot for the surface to surface contact method

#### 6. **Stitch edge**

This method is located in the NX FEM module, and it stitches edges and surfaces together. This test was not successful due to the edges not being close or making contact with each other.

#### 7. **Contact mesh**

This method is located in the NX FEM module and defines a gap mesh, creating elements in between called *CGAP*. The procedure for creating it is to select face pairs, but in this case it did not work due to the surfaces being irregular.

### **Slider test results**

A summary of the results is displayed in **Table 4.4**. As conclusion of the slider test, only three simulations out of seven methods had proper results. Most of the simulations that failed were due to the irregular and complex shape of the crane telescopic parts, or related to the gap being too large.

The mesh mating simulation took the highest simulation time, and as explained previously, it is not accurate since it adds material in an irregular way between the parts, causing the model to lose accuracy regarding to its real counterparts. RBE connection has similar results to Surface to surface gluing, but the simulation time duplicates. Therefore, the slider joint strategy that will be applied for the following tests is the surface to surface gluing.



Test number	Slider joint strategy	Simulation Time [s]	Displacement [mm]	
1	Slider constraint	-	-	
2	Mesh mating	1007	6.872	
3	RBE connection	581	25.83	
4	Surface to surface gluing	282	25.54	*
5	Surface to surface contact	-	-	
6	Contact mesh	-	-	
7	Stitch edge	-	-	

**Table 4.4:** Results for slider joint validation tests

### 4.3.3 Hydraulic cylinders

The Palfinger crane has 10 hydraulic cylinders that move the crane, as shown in **Figure 4.16**, where the parts number 1 and 2 define the crane angle, and the rest define the position of the telescopic parts.

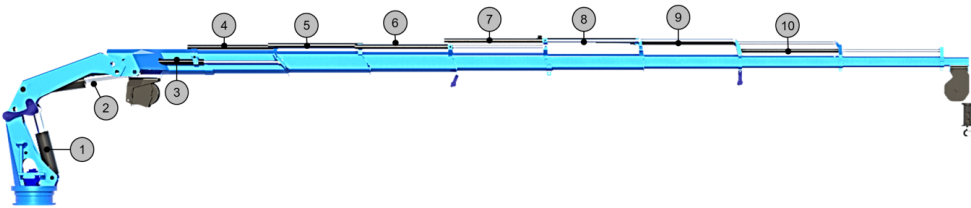


**Figure 4.16:** Hydraulic cylinders

As mentioned previously, for this structural analysis it was considered that the hydraulic cylinders were strong enough to carry all the operations within the product specification limits, consequently they were neglected for the initial complete structural simulation model.

After this model was tested using the revolute and slider joint methods validated previously, it was noted that without hydraulic cylinders the model presented very high displacement results, concluding that the neglected cylinders provided extra support to the structure.

In order to test the previous statement, a set of *superelements* was added to the models with a defined diameter and materials, representing each of the hydraulic cylinders using beam elements, displayed in blue color in **Figure 4.17**. These cylinders are connected to the mesh by a connection with a pin in the case of revolute joints, and to the geometry using a 1D-element connection. Finally, the results were compared to the original model that has no hydraulic cylinders.

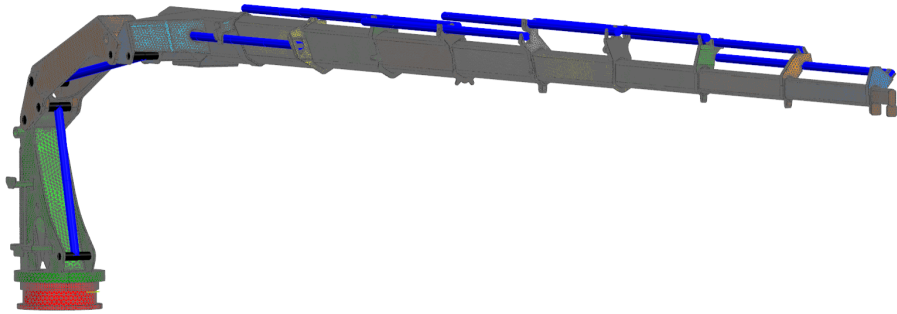


**Figure 4.17:** Hydraulic cylinders modeled as *superelements*, displayed as solids in NX FEM

The tests are defined as following:

1. **Revolute joint model**

For this first comparison, the cylinders 1 and 2 were modeled exclusively for the revolute joints. **Figure 4.18** shows the results for the model without the cylinder. As observed in the stress results in **Figure 4.18b**, there is a stress concentration in the part number 3.

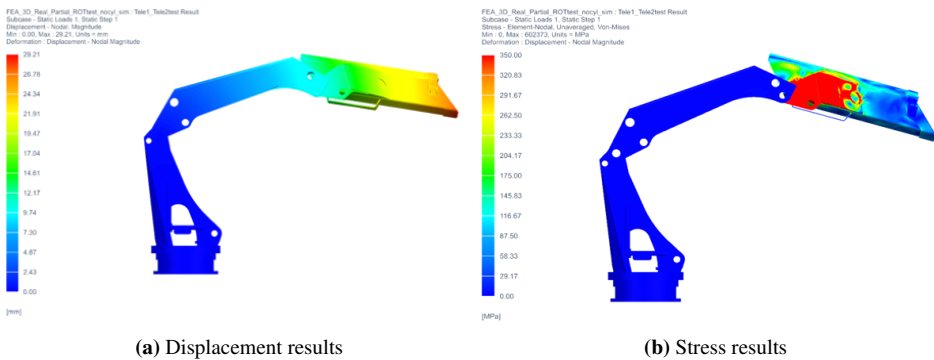


**Figure 4.18:** Revolute model without hydraulic cylinders

In contrast, the model that was tested with hydraulic cylinders is shown in **Figure 4.19**, where the lines across the joints represent the *superelements*.

The stress results displayed in **Figure 4.19b** show a more realistic stress distribution around the revolute joints. As an additional observation, the displacement was reduced considerably.

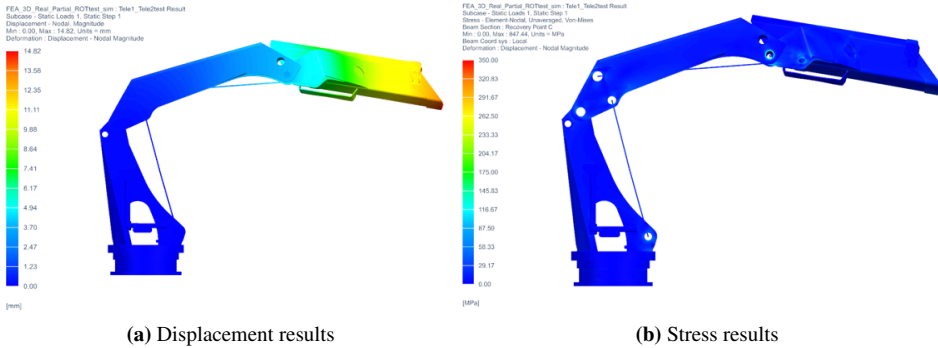


**Figure 4.19:** Revolute model with hydraulic cylinders

## 2. Partial model

In this comparison using the partial model, the cylinders 1 to 6 were modeled, 2 cylinders for the revolute joint and 4 cylinders for the slider joints.

**Figure 4.20** shows the model without any hydraulic cylinders. As observed in the stress results in **Figure 4.20b**, the two revolute joints have a stress concentration.

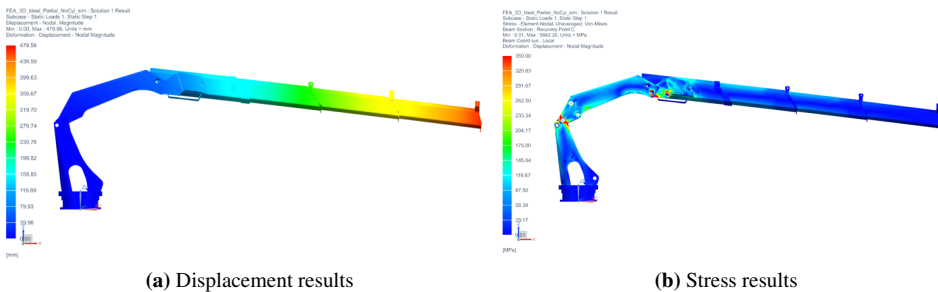


**Figure 4.20:** Partial model without hydraulic cylinders

In **Figure 4.21**, the partial model with 6 modeled cylinders is displayed. The cylinder lines can be observed, which positions were defined by the coordinates of the original 3D hydraulic cylinder models.

The stress results displayed in **Figure 4.21b** show considerably less stress around the revolute joints, and the displacement was reduced considerably.

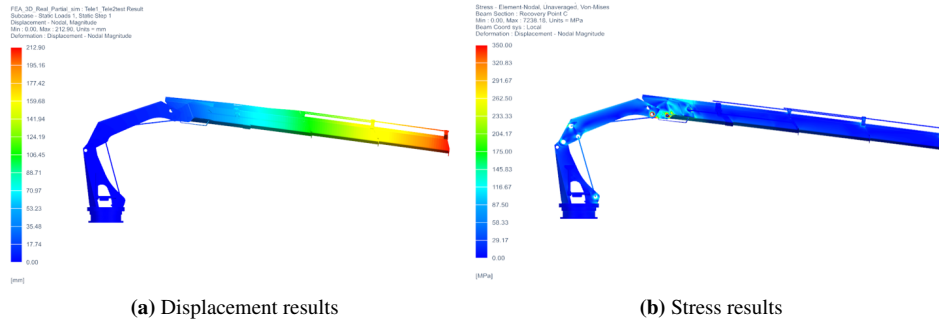


Figure 4.21: Partial model with hydraulic cylinders

### 3. Complete model

In this comparison using the complete model, all the cylinders were added, 2 for the revolute joint and 8 for the slider joints. **Figure 4.22** shows the model without any hydraulic cylinders. As observed in the stress results in **Figure 4.22b**, all the connections between the parts, both revolute and sliders, show a higher stress where the parts make contact.

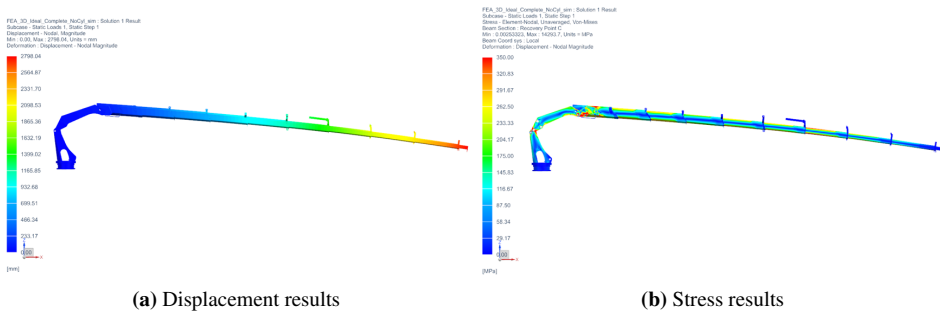
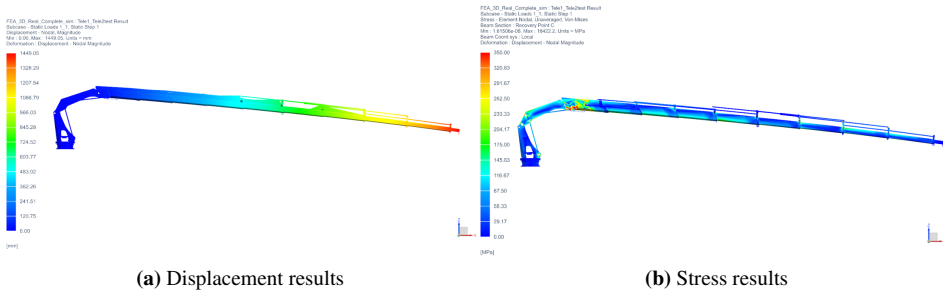


Figure 4.22: Complete model without hydraulic cylinders

In **Figure 4.23**, the complete model with 10 modeled cylinders is displayed. In contrast with the previous stress plot, **Figure 4.23b** shows the stress zones particularly where the telescopic parts make contact, and there is less stress around the revolute joints.

As an additional observation, **Figure 4.24** shows the stress plot from the complete model with the hidden cylinders, to show the stress in the areas where the cylinders are assembled.



**Figure 4.23:** Complete model with hydraulic cylinders

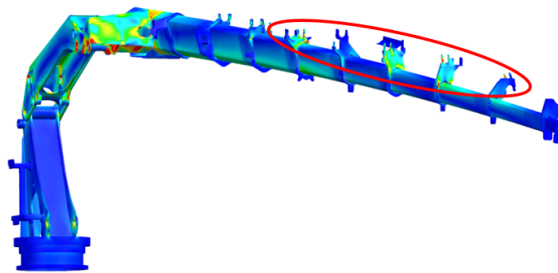


**Figure 4.24:** Stress plot of the complete model with the cylinders (hidden)

### Hydraulic cylinder test results

A summary of the results is displayed in **Table 4.5**. Some important aspects to comment are the impact of the cylinders in relation to the simulation time. Adding the 10 hydraulic cylinders increased the complete model simulation time by a 720%. With the extra-support provided by the cylinders, the displacement was reduced by half. The model without cylinders does not offer an accurate representation of the crane operation, neither for the displacement or stress distribution. Therefore, even if the simulation time increases considerably, adding the hydraulic cylinders increases the accuracy of the model.

Test number	Test strategy	Simulation Time [s]	Displacement [mm]	
1	No-cylinders	235	29.21	
	With cylinders	300 ↑ 128%	14.82 ↓ 51%	★
2	No-cylinders	700	479.56	
	With cylinders	900 ↑ 128%	212.90 ↓ 45%	★
3	No-cylinders	1500	2798.04	
	With cylinders	10800 ↑ 720%	1449.05 ↓ 52%	★

**Table 4.5:** Results for the hydraulic cylinder test

### 4.3.4 Geometry Idealization

With the purpose of reducing the simulation time to increase the model efficiency, a new 3D model was created using the strategy of idealizing the parts. This process cleans up the original model, reducing complex operations and unnecessary features for the structural analysis, as observed in **Figure 4.25**. Some of the tools used for this purpose were *geometry optimization* and deleting faces. The tests and results will be displayed in the next section.

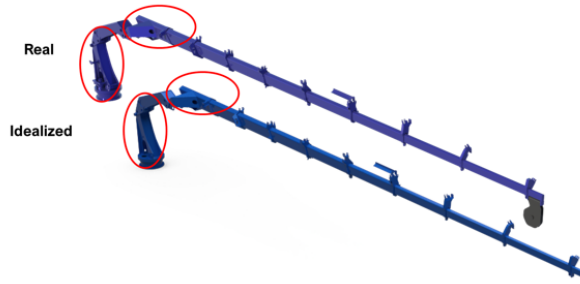


**Figure 4.25:** Real model and the idealized part model

### 4.3.5 Validation tests conclusion

In this section, several tests were developed with the purpose of obtaining the best practices to build up the most accurate and efficient models. For the revolute joint, the most efficient way to model this degree of freedom is to use a C-beam and RBE3 connection in the NX FEM module. For the slider joint, surface to surface gluing will be used, and it is in the NX Sim module. For the hydraulic cylinders, even if they increase considerably the simulation time, the result obtained using them is closer to reality. Finally, the geometry idealization model was developed and will be tested in the next section.

## 4.4 Tests using Finite Element Method

This section applies all the best practices obtained from the validation tests, to build up partial, complete models, and test simplification methods, with the objective of obtaining the most accurate and efficient model. The test plan is displayed in **Figure 4.26** and begins with testing the 3D models: both real and idealized, using the complete and partial models. After that, a partial simplification of the crane using 2D shell elements will be attempted, to finalize with two different simplifications using 1D elements. It is important to mention that all the tests were done with two different load values: 5 kN and 20 kN, and only the 20 kN results will be discussed in this section, since it is the maximum load that the crane can carry at current position. The 5 kN tests and results can be found in the appendix 8.1.

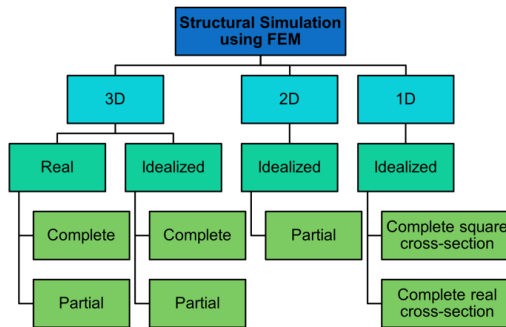


Figure 4.26: Test plan for the structural simulation

### 4.4.1 3D Elements

This section will compare the real model results with the idealized model, for both partial and complete configurations. The element type used in the following simulations is *CTetra(10)* for all the 3D simulations. In addition, the results that will be used as reference are the real model results.

#### Partial 3D model test

The first configuration to be tested will be the partial, where **Figure 4.27** shows the displacement, stress and glue plots for the real model and **Figure 4.28** shows the results for the idealized model.

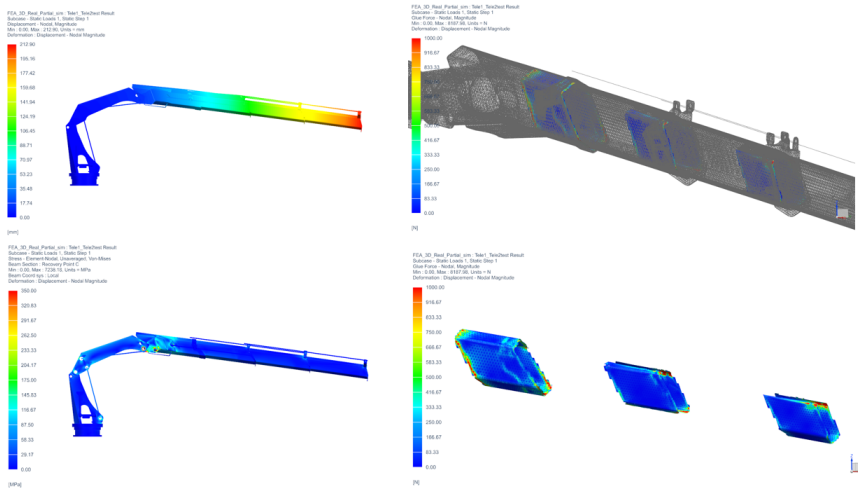


Figure 4.27: 3D Real Model - Partial Test at 20 kN result

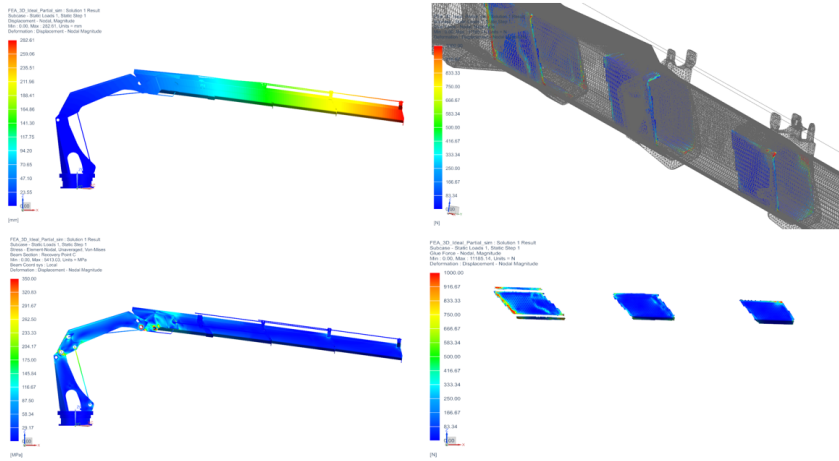


Figure 4.28: 3D Ideal Model - Partial Test at 20 kN result

### Complete 3D model test

The second configuration to be tested is the complete model, where **Figure 4.29** shows the displacement, stress and glue plots for the real model and **Figure 4.30** shows the results for the idealized model.

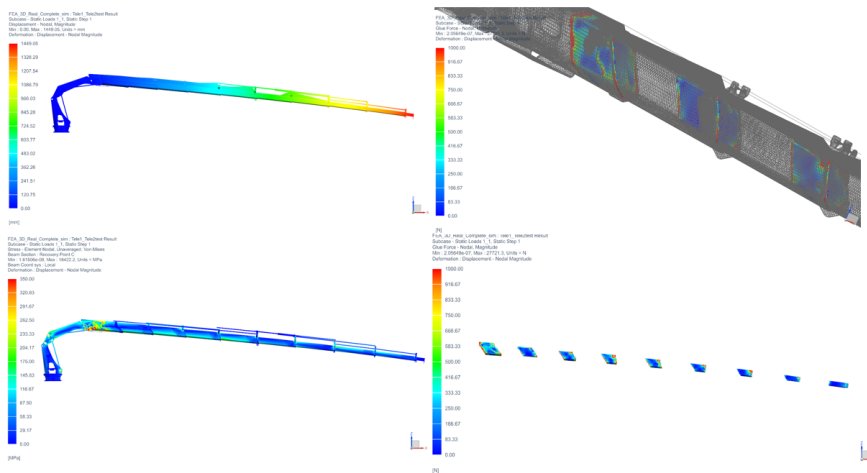
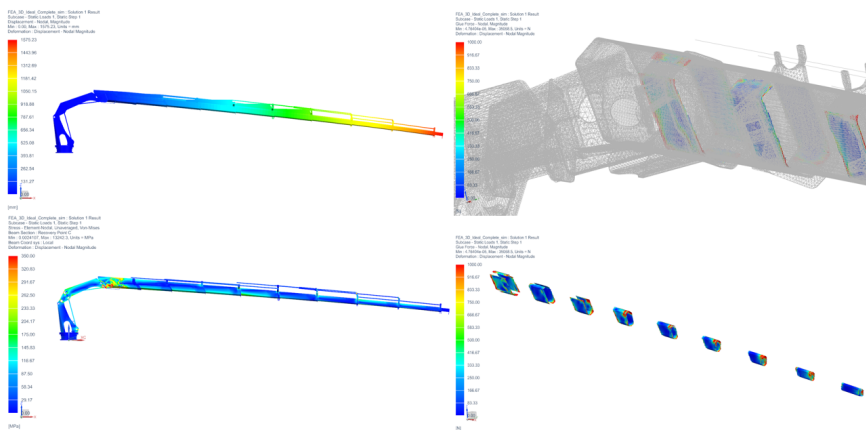


Figure 4.29: 3D Real Model - Complete Test at 20 kN result





**Figure 4.30:** 3D Ideal Model - Complete Test at 20 kN result

### 3D tests summary

**Table 4.6** shows the results for the partial test, where the simulation time using the idealized model was reduced by a 20% while increasing the displacement variation to 33%.

Test number	Model configuration	Simulation Time [s]	Displacement [mm]
1	Real partial	900	212.9
2	Ideal partial	720 ↓ 20%	282.61 ↑ 33%

**Table 4.6:** Results for partial tests at 20 kN

As observed when comparing the plots, the two complete models behave in a very similar way. The glue plots show the forces increasing in the same areas, and the stress is distributed in the same way. **Table 4.7** shows the results for this test, where the simulation time using the idealized model was reduced by a 42% while increasing the displacement variation to 9%.

Test number	Model configuration	Simulation Time [s]	Displacement [mm]
1	Real complete	10800	1449.05
2	Ideal complete	6300 ↓ 42%	1575.23 ↑ 9%

**Table 4.7:** Results for complete tests at 20kN

The idealization of the 3D model did have a positive impact reducing considerably the simulation time, while adding variation in the displacements. This model can be refined to reduce both the simulation time and the displacement error.

### 4.4.2 2D Shell Elements

A 2D shell model was developed using as a reference model the 3D ideal model and simplifying it by using the tool *midsurface* to create a thin layer that would represent the crane, part by part. This model is displayed in **Figure 4.31**.

When developed, it was necessary to connect every surface using tools as *stitch edge* or *sew*, making this model extremely time-consuming due to the complexity of the crane's geometry. Therefore, several attempts were made to create an accurate 1D model.

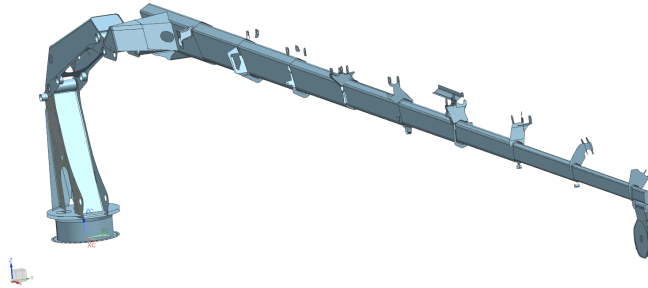


**Figure 4.31:** 2D Shell of the crane

### 4.4.3 1D Beam Elements simplification

With the purpose of testing the accuracy and solving time of the 1D beam simulations, a representation of the 3D model was developed. This means that every part was reduced to a line with a definite set of nodes, a specified cross-section and material properties. **Figure 4.32** shows the 1D model with the real cross-section and solid aspect representation, next to the 3D real model.

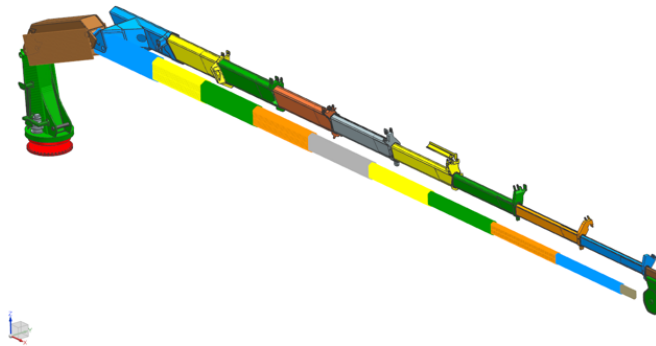


**Figure 4.32:** 1D model using the solid visualization in comparison with the 3D real model

For this section, two different simplification models were created, they are shown in **Figure 4.33**. The difference between the models is the detail of the telescopic parts. The first model created was using a square cross-section with the approximate sizes of the parts, and is displayed in **Figure 4.33a**, while the second model was defined using the accurate cross-sections for the telescopic parts, displayed in **Figure 4.33b**.

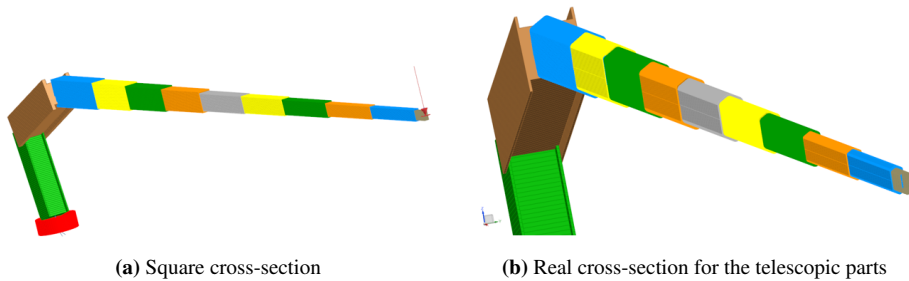


**Figure 4.33:** 1D approximation models with different cross-sections

### Square cross-section Test

The objective of this test is to compare the results and simulation time obtained by using a 1D simplified square cross-section model with the 3D real model. **Figure 4.34** shows the displacement and stress plots for this model.

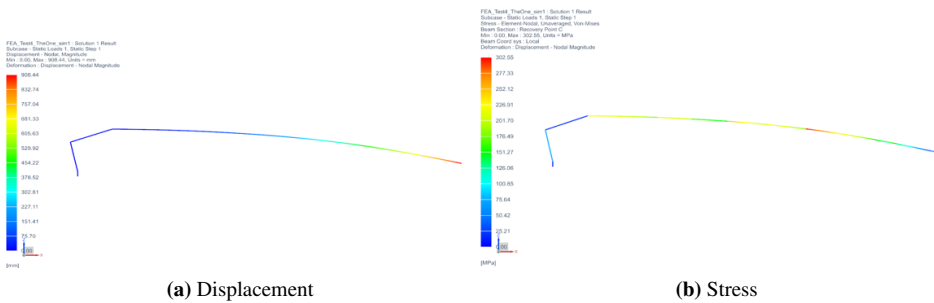


**Figure 4.34:** 1D square cross-section approximation test results at 20 kN

### Real cross-section approximation

For this approximation, the real cross-section was extracted part by part from the telescopic models, and used as input to define the shape and thickness of the parts. **Figure 4.35** shows the displacement and stress results for this model.

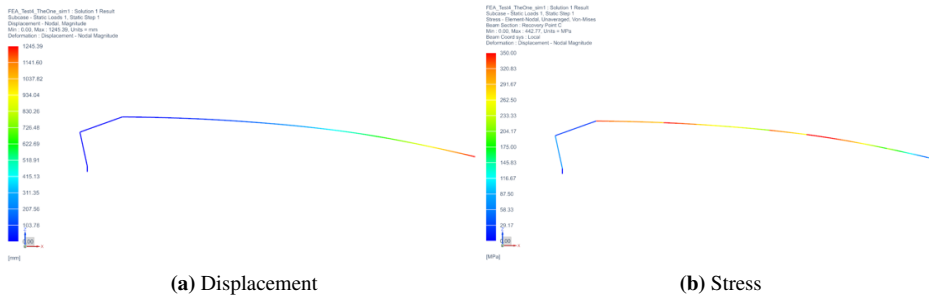


**Figure 4.35:** 1D real cross-section approximation test results at 20 kN

### 1D beam approximation tests summary

As observed in the previous plots, the elements appear as 1D beams which have particular properties. The summary of the results is displayed in **Table 4.8** which the simulation time was surprisingly reduced to 0.5 seconds for both models. The displacement shows a considerable variation from the square cross-section to the real cross-section. The fact that this simulation can run almost in real-time, makes it suitable for a digital twin application, but it requires further verification and refinement.

Test number	Model configuration	Simulation Time [s]	Displacement [mm]
1	Square cross-section	0.5	908.44
2	Real cross-section	0.5	1245.39

**Table 4.8:** Results for complete 1D tests at 20kN

## 4.5 Results summary

As a summary of the tests documented in the previous sections, **Table 4.9** documents the results for 20 kN. For the results using 5 kN, see appendix 8.1.5. The items marked with stars will be discussed. For the percentage comparison, it is important to define the 3D complete real model as reference.

The idealized model was successful reducing the simulation time, varying from a 20% to a 42% reduction, while the 1D model was able to reduce this value by a 99%. As observed in the results table, the 3D ideal model presents a displacement variation of the 9% in contrast with the real model. Comparing with the 1D model, this displacement variation goes up to 14%. As further work, it is important to refine the 1D model to be able to generate accurate results in a simulation time of less than one second.

Test	Model	Configuration	Displacement [mm]	Simulation time [s]	
1	3D Partial	Real	212.9	900	
		Idealized	282.61 $\uparrow 33\%$	720 $\downarrow 20\%$	
2	3D Complete	Real	1449.02	10800	★
		Idealized	1575.23 $\uparrow 9\%$	6300 $\downarrow 42\%$	
3	1D Complete	Square	908.44 $\downarrow 37\%$	0.5 $\downarrow 99\%$	
		Real	1245.39 $\downarrow 14\%$	0.5 $\downarrow 99\%$	★

**Table 4.9:** Structural simulation test results summary for 20 kN

## 4.6 Suggested strain gauge sensor locations

With the previous simulations, it is possible to define suggested locations for installing the strain gauges in the physical crane. Four locations have been selected according to the simulation results on the crane structure.

**Figure 4.36** shows the crane from a front perspective using three different simulations: 3D real, 3D ideal and 1D with real cross-section. Some observations from this figure are the stress distribution from the location 3 and 4 changes to be located in the lower side of the structure, to be on the upper part.

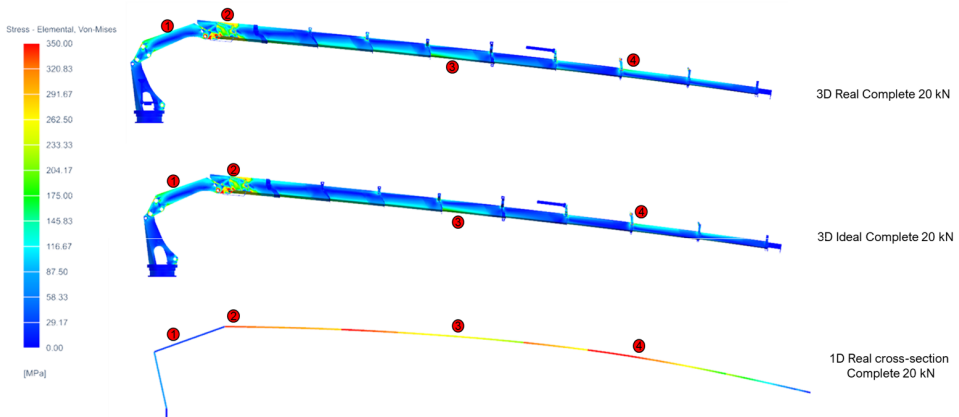


**Figure 4.36:** Suggested strain gauge locations and stress plots in a front perspective

In **Figure 4.37**, the 3D results are displayed in a top perspective, showing a different stress distribution. An important observation is that the crane presents a rotation, which can be compared with the red line.

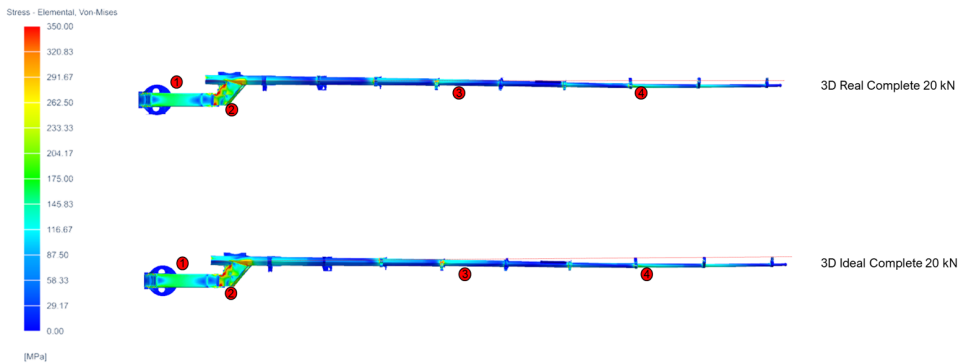


**Figure 4.37:** Suggested strain gauge locations and stress plots in a top perspective

The sensor location was selected according to the following data:

1. The first sensor was defined as mounted in the part number 3, due to being one of the main structural parts that defines angles.
2. The second sensor is mounted in the part number 4, which presents some red areas according to the stress plots, and is also one of the fundamental parts that will be changing the angles.
3. The third sensor is located in the part number 8 in the bottom, and it has a telescopic movement. It was chosen since it had the highest stress among the telescopic parts.
4. The fourth sensor is located in the part number 11, since the stress distribution changes from the bottom to the top. It is also important to monitor the stress across several spaced points in the structure, particularly since rotation has been noted.

## 4.7 Flexible Body Sim and preparation for the Digital Twin

For the connection between the structural and the kinematic simulations, a particular flexible body simulation was made to ensure the compatibility of the results. The crane part selected for this test was the part number 3, since it is one of the key structural components receiving loads.

A flexible body simulation is used for the kinematic analysis of a mechanism, calculating natural frequencies and modes of the mechanical parts. [24] It can be used as input for the kinematic motion simulation.

The process for creating this part is the same than a FEA analysis until the meshing part. It is built using the NX FEA module, where in addition to the mesh, a set of points need to be added to the part, according to how they are assembled in the kinematic simulation. These points are added and connected using RBE2 collectors, as displayed in **Figure 4.38**

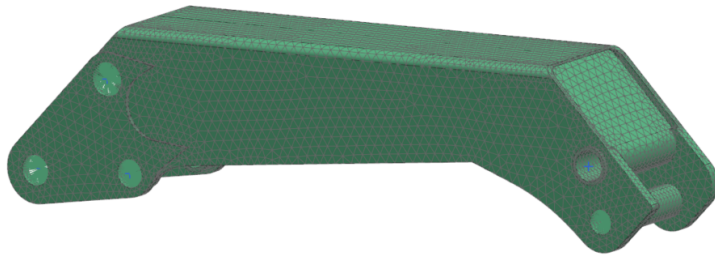


**Figure 4.38:** NX FEM model with the assembly points for a flexible body simulation

The next step was to create a simulation selecting the solution type as *SOL103 Flexible Body* in the NX Sim module, and add the constraints to the points that were added to the mesh in the NX FEM module. This step is particularly important since the constraint type is *Fixed DOF*, and depending on the degrees of freedom of the part, it can be customized as fixed or free. In this case, all the points are fixed, so five *Fixed DOF* constraints were created.

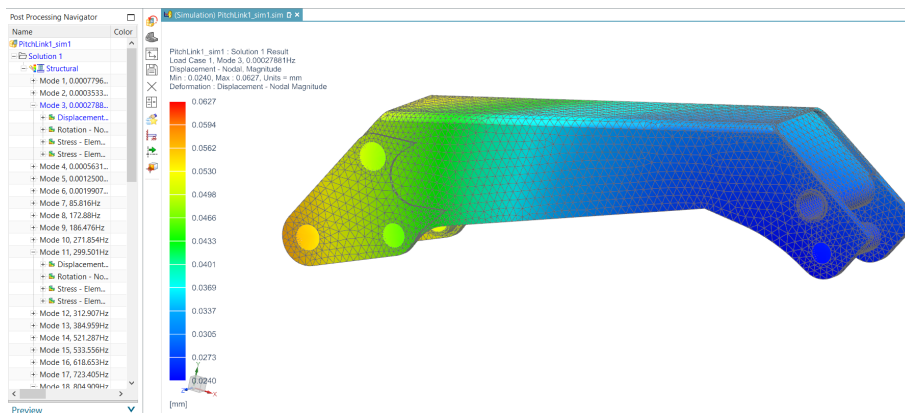


**Figure 4.39:** NX Sim results showing a set of result modes for the same part

The last step is to solve the model. The output of the simulation is displayed in **Figure 4.39**, where a set of modes are calculated. This simulation takes approximately 600 seconds, a considerable amount of time, since it evaluates several modes or eigenvalues specified. This structural simulation results will be used in the digital twin model.





# Kinematic Simulation

In this section, the methodology followed for developing the kinematic simulation of the maritime crane using NX will be detailed. The first step was to define the model and the crane operation, then the motion bodies and joints were defined, followed by the implementation of control. It is important to explain that for every test, the simulation-based design methodology was applied. The particular NX module used for every step is shown in **Figure 5.1**.

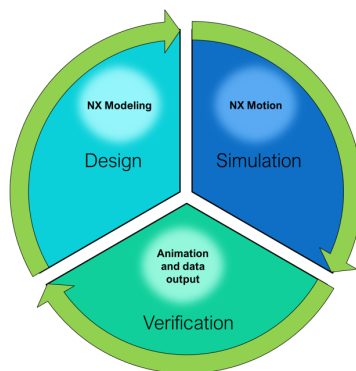


**Figure 5.1:** Simulation-based design diagram for the kinematic simulation

For the design phase, NX Modeling will be used to modify the model and parts for the test scenario. The simulation phase will be developed in NX Motion, where all the links and joints will be defined and simulated. The verification phase will be evaluated with the animation, data plots and spreadsheets. With this verification, the model will be improved as necessary for the next iteration.

## 5.1 Model selection and considerations

The first step into developing the kinematic simulation is to define the model that will be used. In this case, it is important to consider the weight of the parts, therefore the complete original model was selected, displayed in **Figure 5.2**, with the exception of the wire model, since it will be simulated with functions.



**Figure 5.2:** Kinematic Model

An important consideration for the kinematic motion simulation is that the cylinders will be treated only as mechanical components, not as hydraulic parts. NX Motion is able to simulate hydraulic cylinders by using functions and plots, but for this case, since the information on the cylinders was limited, it was not possible to include them in the simulation. Therefore, the revolute and slider joints are controlled by drivers that simulate the crane degrees of freedom.

Regarding the simulation time, for this case it was mostly not recorded since it changes abruptly according to parameters such as 3D contact, motion driver and control parameters. In addition, as stated previously in the section 3.1.2, the data input for this simulation will be created.

### 5.1.1 Crane Joints

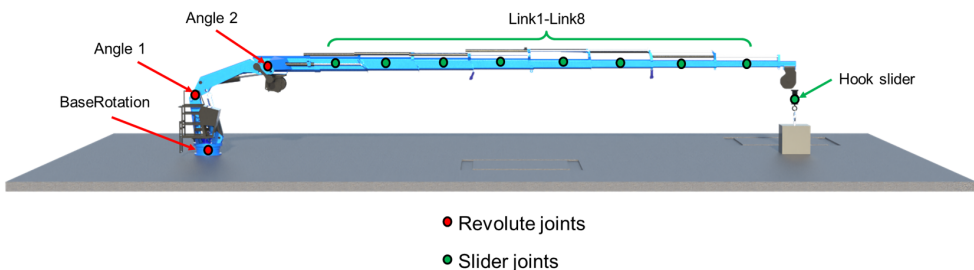


**Figure 5.3:** Joints for the kinematic model

The crane joints were previously explored in section 3.3, consisting of 3 revolute joints and 9 sliders. For simplification purposes, the final telescopic part was considered as fixed,

since it does not have a particular hydraulic cylinder that operates it. **Figure 5.3** shows the final kinematic model and the joints for this simulation, 3 revolute joints are considered and 9 slider joints, where 8 belong to the telescopic parts, and the last one corresponds to the crane hook that moves the load up and down.

## 5.2 Crane Operation

The desired simulation output is defined as the crane lifting a load or box with a current mass of 2 tons, move joint by joint to reach the position A and then the position B, as displayed in **Figure 5.4**.

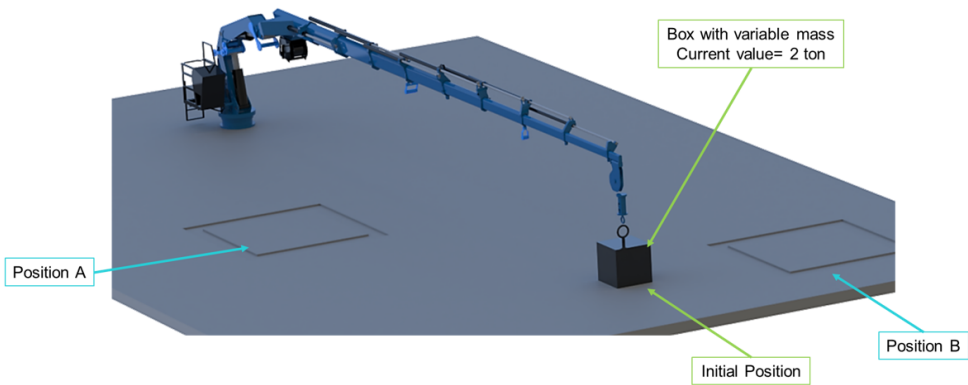


**Figure 5.4:** Test scenario for the kinematic simulation

After calculating the variables to reach the positions, the step-by-step operations are determined as following:

1. *HookSlider* lifts the load
2.  $Angle1 = -5^\circ$
3.  $Angle2 = -10^\circ$
4. From *Link8* to *Link1* the values move gradually to the minimum length
5.  $BaseAngle = -20^\circ$
6.  $Angle2 = 0^\circ$
7. From *Link1* to *Link8* the telescopic parts expand to reach Position A
8.  $Angle1 = 0^\circ$

9. *HookSlider* releases the load
10. 5 seconds after, *crane hook* lifts the load
11.  $Angle1 = -5^\circ$
12.  $BaseAngle = 15.9^\circ$
13. From *Link1* to *Link8* the telescopic parts expand to reach Position B
14.  $Angle1 = 0^\circ$
15. *HookSlider* releases the load

As noted in the step-by-step operations, the order of movement for the telescopic parts is important, since the real crane behavior is controlled by the cylinders. In addition, the reason behind the selection of this particular operation is first, to test all the joints separately, and second to evaluate the load impact on the parts when the box is lifted and released.

## 5.3 Motion model setup

In this section, the crane model will be used to replicate the crane behavior using NX Motion. As observed in previous screenshots, several parts were designed to be able to run the simulation, such as the floor with position markers and the load with a variable mass.

### 5.3.1 Motion Bodies

The first step for the motion simulation, is to define the motion bodies. The purpose of this step is to select the parts that will move and define their mass and inertia, which can be defined automatically or user defined. In addition, the program allows the selection of initial translation or rotation velocities, and the option to fix the body. As an example, the floor part was the only motion body which was defined as fixed.

### 5.3.2 Joints

The second step is the definition of joints, which will define how the parts will move in relation to other motion bodies. For each joint, two parts need to be selected to define the relative movement between them. The joint types used were only revolute and slider, which require the selection of a shared axis, and the limits. **Figure 5.5** shows the selection window for a slider joint creation, with the defined limits. In the same menu, the friction and driver options can be specified. For this kinematic simulation the friction was disabled and the driver configuration will be detailed in the next section.

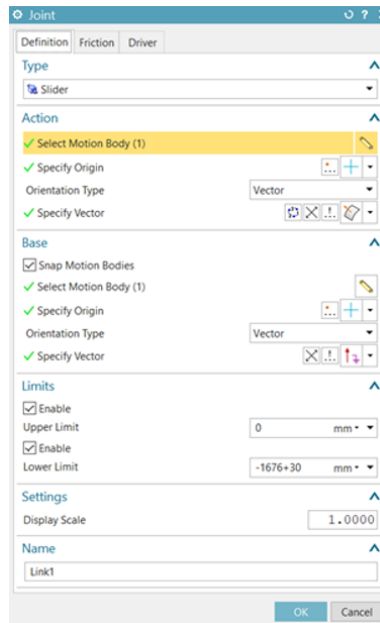


Figure 5.5: Joint limit configuration for the *link1* slider

### 5.3.3 Drivers

The drivers control the joints among its already defined limits, both for rotation and translation. The driver types that will be tested for the development of the kinematic simulation using NX Motion are:

- **Polynomial**  
Defines the movement by an initial displacement, velocity, acceleration and jerk.
- **Harmonic**  
Defines the movement by setting up the amplitude, frequency, phase angle and displacement values. **Figure 5.6** shows the menu for the driver setup.

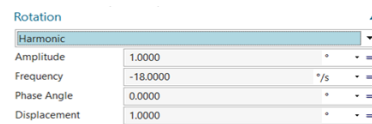
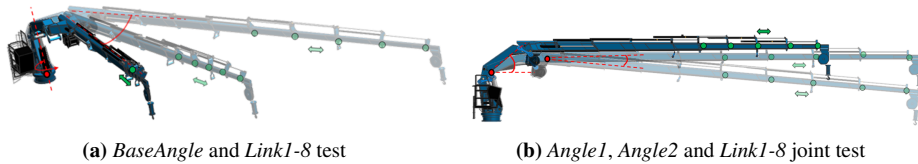


Figure 5.6: Harmonic Driver setup for a revolute joint

- **Profile 2D**  
Defines the movement by the selection of a 2D data set, such as a spreadsheet, allowing the control of the variables.

Several tests were made for each joint, initially using only polynomial and harmonic drivers. Figure **Figure 5.7** depict several frames of an animation where the joints were tested. The polynomial and harmonic drivers are designed for a cyclical or repetitive operation, but for the crane case it was not possible to simulate the complex operation using those drivers. Therefore, they were useful for validation purposes, and small test scenarios. The final model will use the Profile 2D and it will be detailed in the motion control section.



**Figure 5.7:** Joints test

### Expressions

The NX Expressions tool was programmed for the polynomial and harmonic drivers, as shown in **Figure 5.8**. This tool allows all the programmed variables to be changed in the same location, reducing the testing time.

Name	Formula	Value	Units	Dimensionality	Type
Angle1_Acceleration	0	0 °/s <sup>2</sup>	°/s <sup>2</sup>	Angular Accel...	Number
Angle1_InitialDisplacement	10	10 °	°	Angle	Number
Angle1_Jerk	0	0 °/s <sup>3</sup>	°/s <sup>3</sup>	Angular Jerk	Number
Angle1_Velocity	-1.5	-1.5 °/s	°/s	Angular Velocity	Number
Angle2_Acceleration	0	0 °/s <sup>2</sup>	°/s <sup>2</sup>	Angular Accel...	Number
Angle2_InitialDisplacement	-5	-5 °	°	Angle	Number
Angle2_Jerk	0	0 °/s <sup>3</sup>	°/s <sup>3</sup>	Angular Jerk	Number
Angle2_Velocity	1.5	1.5 °/s	°/s	Angular Velocity	Number
BaseAngle_Acceleration	0	0 °/s <sup>2</sup>	°/s <sup>2</sup>	Angular Accel...	Number
BaseAngle_InitialDisplacement	0	0 °	°	Angle	Number
BaseAngle_Jerk	0	0 °/s <sup>3</sup>	°/s <sup>3</sup>	Angular Jerk	Number
BaseAngle_Velocity	0	0 °/s	°/s	Angular Velocity	Number
Link1_Acceleration	0	0 mm/s <sup>2</sup>	mm/s <sup>2</sup>	Acceleration	Number
Link1_InitialDisplacement	-1676+30	-1646 mm	mm	Length	Number
Link1_Jerk	0	0 mm/s <sup>3</sup>	mm/s <sup>3</sup>	Jerk	Number
Link1_Velocity	120	120 mm/s	mm/s	Velocity	Number
Link2_Acceleration	0	0 mm/s <sup>2</sup>	mm/s <sup>2</sup>	Acceleration	Number
Link2_InitialDisplacement	-1829.7+30	-1799.7 mm	mm	Length	Number
Link2_Jerk	0	0 mm/s <sup>3</sup>	mm/s <sup>3</sup>	Jerk	Number
Link2_Velocity	120	120 mm/s	mm/s	Velocity	Number

**Figure 5.8:** Driver setup for all variables programmed using NX expressions

### 5.3.4 3D Contact

For the crane motion simulations, there are several parts that require to be modeled as 3D contact. Since 3D contact is a heavy simulation tool, its use was reduced to only the necessary components:

1. Contact between the crane hook and the load
2. Contact between the load and the floor
3. Contact between the angular cylinders and pistons

#### Model improvement

The original crane hook was modified to provide a better grip, since there were cases where the crane hook would drop the load due to its shape, and it impacted the simulation time considerably. **Figure 5.9** shows the model before and after the 3D model improvement.

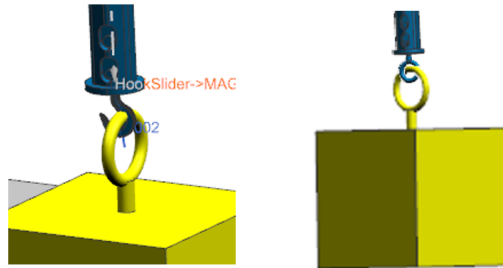


**Figure 5.9:** Initial hook model and improved version, to reduce the 3D contact computation time

As commented previously, in the motion simulation, the computing time varies abruptly according to several parameters, but for the crane hook improvement, a completely identical simulation was able to show the differences between the two models. The results are displayed in **Table 5.1**, obtaining a reduction of the 92% in the simulation time.

Test	Hook type	Simulation time [s]
1	Original hook	2870
2	Improved hook	240 ↓ 92% ★

**Table 5.1:** Simulation time using different crane hooks and 3D contact

## 5.4 Motion control and preparation for the Digital Twin

In this section, the required control for the crane will be developed with the purpose of achieving the operation specified previously. The method for controlling the crane actua-

tors is called *2D Profile* since it allows the use of an excel spreadsheet as an input. This function will be valuable when connecting the real data from the sensors mounted in the crane. For this operation, the input data will be simulated by the use of a spreadsheet with the calculated values.

### 5.4.1 List of inputs for the motion sim

The first step towards setting up the motion control is to define the necessary inputs for the simulation. This is an important step since it needs to consider the connection with the physical crane. **Table 5.2** defines the variables that need to be received by the simulation, together with its maximum and minimum values. With this data, the crane operation can be simulated using an excel spreadsheet.

Joint	Name in Excel spreadsheet	Variable name in NX	Max. value	Min. value
1	Angular displacement (°)	<i>Angle1</i>	-40°	40°
2	Angular displacement 2 [°]	<i>Angle2</i>	-25°	25°
3	Base Angular [°]	<i>BaseRotation</i>	No limit	No limit
4	Link1, slider [mm]	<i>Link1</i>	-1460.94	30
5	Link2, slider [mm]	<i>Link2</i>	-1629	30
6	Link3, slider [mm]	<i>Link3</i>	-1730	30
7	Link4, slider [mm]	<i>Link4</i>	-1970	30
8	Link5, slider [mm]	<i>Link5</i>	-1852	150
9	Link6, slider [mm]	<i>Link6</i>	-1963	120
10	Link7, slider [mm]	<i>Link7</i>	-2020	120
11	Link8, slider [mm]	<i>Link8</i>	-2025	120
12	HookSlider [mm]	<i>HookSlider</i>	465.314	350

**Table 5.2:** List of inputs for the motion simulation using a Profile 2D control

### 5.4.2 Simulation of Data Input

The objective of this section is to design and calculate the data to achieve the previously mentioned crane operation. It was entirely developed using Excel, with some measurements and calculations taken from NX Modeling and Motion. The simulation duration will be of 283 seconds, with a time-step of 0.1 seconds. These parameters are critical when developing the data spreadsheet, since it needs to fit exactly the amount of items and step sizes.

**Figure 5.10** shows the excel spreadsheet input screenshot, with the variables listed in the previous section. In addition, the time-step of the simulation can be observed.



## 5.4 Motion control and preparation for the Digital Twin

Time (s)	Angular Displacement (deg)	Base Angular Displacement (deg)	Link1_slider (mm)	Link2_slider (mm)	Link3_slider (mm)	Link4_slider (mm)	Link5_slider (mm)	Link6_slider (mm)	Link7_slider (mm)	Link8_slider (mm)	HookSlide
0.000	1.000	15.900	30.000	30.000	30.000	30.000	150.000	120.000	120.000	120.000	760.000
0.100	0.900	15.900	30.000	30.000	30.000	30.000	150.000	120.000	120.000	120.000	750.577
0.200	0.800	15.900	30.000	30.000	30.000	30.000	150.000	120.000	120.000	120.000	741.163
0.300	0.700	15.900	30.000	30.000	30.000	30.000	150.000	120.000	120.000	120.000	731.768
0.400	0.600	15.900	30.000	30.000	30.000	30.000	150.000	120.000	120.000	120.000	722.400
0.500	0.500	15.900	30.000	30.000	30.000	30.000	150.000	120.000	120.000	120.000	713.079
0.600	0.400	15.900	30.000	30.000	30.000	30.000	150.000	120.000	120.000	120.000	703.796
0.700	0.300	15.900	30.000	30.000	30.000	30.000	150.000	120.000	120.000	120.000	694.557
0.800	0.200	15.900	30.000	30.000	30.000	30.000	150.000	120.000	120.000	120.000	685.393
0.900	0.100	15.900	30.000	30.000	30.000	30.000	150.000	120.000	120.000	120.000	676.309
1.000	0.000	15.941	30.000	30.000	30.000	30.000	150.000	120.000	120.000	120.000	667.291
1.100	-0.100	15.182	30.100	30.100	30.100	9.990	129.980	99.170	98.610	98.540	658.379
1.200	-0.200	14.823	30.200	30.200	30.200	-10.020	109.960	78.340	77.220	77.080	649.563
1.300	-0.300	14.464	30.300	30.300	30.300	-30.030	89.940	57.510	55.830	55.620	640.898
1.400	-0.400	14.105	30.400	30.400	30.400	-50.040	69.920	36.680	34.440	34.160	632.286
1.500	-0.500	13.746	30.500	30.500	30.500	-70.050	49.900	15.850	13.051	12.700	623.803
1.600	-0.600	13.387	30.600	30.600	30.600	-90.059	29.880	-4.980	-8.339	-8.759	615.474
1.700	-0.700	13.028	30.700	30.700	30.700	-110.069	9.860	-25.810	-29.729	-30.219	607.288
1.800	-0.800	12.669	30.800	30.800	30.800	-130.079	-10.160	-46.640	-51.119	-51.679	599.252
1.900	-0.900	12.310	30.900	30.900	30.900	-150.089	-30.180	-67.470	-72.509	-73.139	591.376
2.000	-1.000	11.951	31.000	31.000	31.000	-170.099	-50.200	-88.300	-93.899	-94.599	583.664
2.100	-1.000	11.592	31.100	31.100	31.100	-190.109	-70.220	-109.130	-115.289	-116.059	576.128
2.200	-1.000	11.233	31.200	31.200	31.200	-210.119	-90.240	-129.960	-136.679	-137.519	568.778
2.300	-1.000	10.874	31.300	31.300	31.300	-230.129	-110.260	-150.790	-158.069	-158.979	561.606
2.400	-1.000	10.515	31.400	31.400	31.400	-250.139	-130.280	-171.620	-179.459	-180.439	554.636
2.500	-1.000	10.156	31.500	31.500	31.500	-270.148	-150.300	-192.450	-200.849	-201.899	547.868
2.600	-1.000	9.797	31.600	31.600	31.600	-290.158	-170.320	-213.280	-222.239	-223.359	541.309
2.700	-1.000	9.438	31.700	31.700	31.700	-310.168	-190.340	-234.110	-243.629	-244.819	534.967
2.800	-1.000	9.079	31.800	31.800	31.800	-330.178	-210.360	-254.940	-265.019	-266.279	528.846
2.900	-1.000	8.720	31.900	31.900	31.900	-350.188	-230.380	-275.770	-286.409	-287.739	522.954
3.000	-1.000	8.361	32.000	32.000	32.000	-370.198	-250.400	-296.600	-307.799	-309.199	517.295
3.100	-1.000	8.002	32.100	32.100	32.100	-390.208	-270.420	-317.430	-329.189	-330.659	511.876
3.200	-1.000	7.643	32.200	32.200	32.200	-410.218	-290.440	-338.260	-350.579	-352.119	506.702
3.300	-1.000	7.284	32.300	32.300	32.300	-430.228	-310.460	-359.090	-371.969	-373.579	501.777
3.400	-1.000	6.925	32.400	32.400	32.400	-450.238	-330.480	-379.920	-393.359	-395.039	497.108
3.500	-1.000	6.566	32.500	32.500	32.500	-470.248	-350.500	-400.750	-414.749	-416.499	492.698
3.600	-1.000	6.207	32.600	32.600	32.600	-490.257	-370.520	-421.580	-436.139	-437.959	488.552
3.700	-1.000	5.848	32.700	32.700	32.700	-510.267	-390.540	-442.410	-457.527	-459.417	484.674
3.800	-1.000	5.489	32.800	32.800	32.800	-530.277	-410.560	-463.240	-478.917	-480.877	481.067

Figure 5.10: Screenshot from the Excel spreadsheet for the data input

### 5.4.3 2D Profile control

This section connects the excel spreadsheet containing simulated data, with the kinematic simulation using the 2D Profile function.

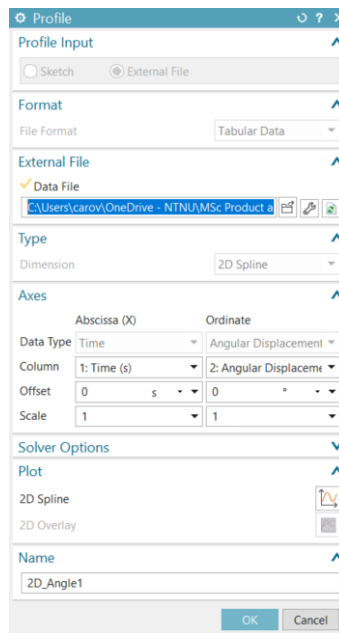
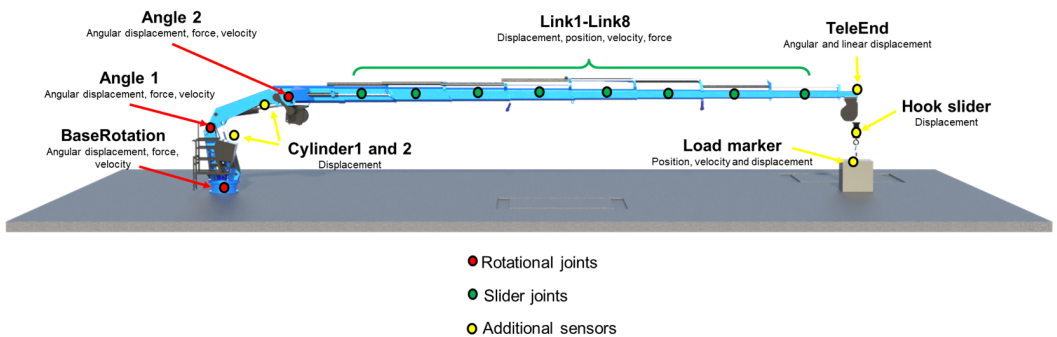


Figure 5.11: 2D Profile Driver configuration window for Angle1

**Figure 5.11** shows the configuration window, which requires a sketch or an external file selection. Once selected, a check-mark will appear if the program finds the correct time column, allowing the selection of the desired variable data. In addition, an offset and scale can be selected for the values.

## 5.5 Sensor locations

Sensors in the NX Motion module can be obtained from joints or variables that are already existing, or create a particular sensor. As observed in **Figure 5.11**, most of the sensors are extracted from the rotational or slider joints and data already simulated, while the additional sensors are the functions that were created to monitor a particular measurement.



**Figure 5.12:** Location of sensors in the crane

### 5.5.1 List of sensors and plots in Data Output

The list of sensors added to the model includes 50 sensors. The tables can be found in section 8.2.1. All of those values can be plotted and simulated in real time. Some data can even be visualized during the animation in real time with colors, in the location of the measurement.

### 5.5.2 Excel spreadsheet output

All the data from the 50 sensors can be extracted step by step into an excel spreadsheet directly from the NX Motion after a simulation is finished. This excel spreadsheet output can be used for the control feedback signal that closes the loop between the real crane and the digital twin. It is important to mention that this file takes a considerable time to generate, since it contains all the data from the 50 sensors step by step, as shown in **Figure 5.13**.

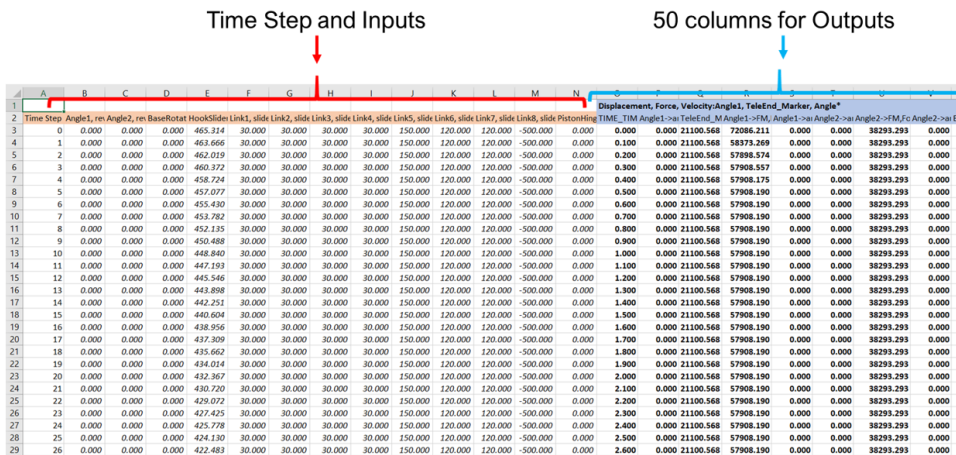


Figure 5.13: Excel Output File with measurements from 50 sensors

## 5.6 Results summary

This simulation provides a series of important results for this project, such as the animation, displayed in **Figure 5.14**, where the crane is moving and the load is swinging, reacting to the movements. In addition, the plots and the connectivity that was enabled by the use of the 2D Profile control, which provides an established data-set that is required to feed the simulation for the digital twin.

A part of the operation involves a pause and releasing the load. This movement and its effects will be seen in the plots around the time-step 180 to 190 approximately.



Figure 5.14: Kinematic Simulation of the maritime crane using NX Motion

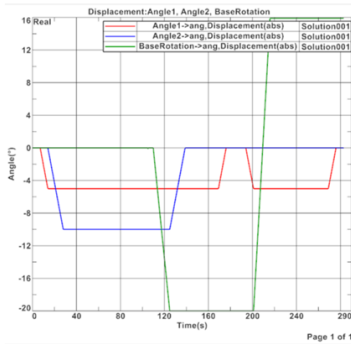
The following results are a set of plots from joints and sensors, providing useful data to compare for when the sensors are mounted on the physical crane.

### 5.6.1 Revolute joints

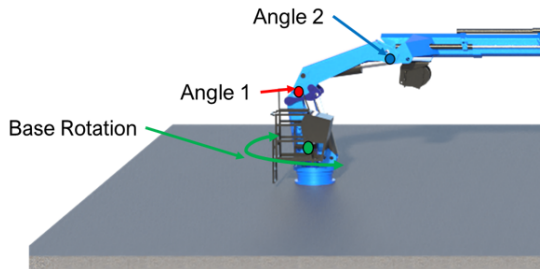
In this section, two different plots are commented using the revolute joints.

#### Angular displacement in the revolute joints

The objective of this test is to verify the revolute joints behavior along the kinematic simulation. The results are displayed in **Figure 5.15**.



(a) Revolute joints plot

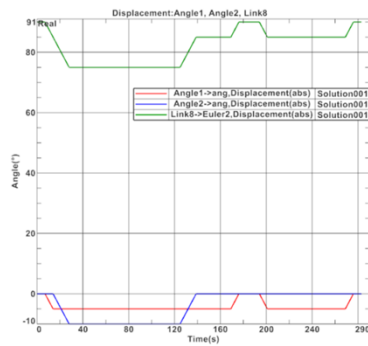


(b) Angle1, Angle2 and BaseRotation displayed in the crane

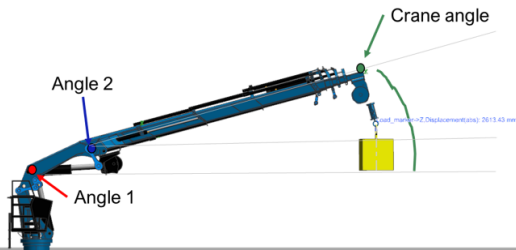
**Figure 5.15:** Revolute joints plot during the kinematic simulation

#### Crane angle

The purpose of this test is to plot and understand how *Angle1* and *Angle2* impact the total crane angle. The results are displayed in **Figure 5.16**.



(a) Angular displacement plot



(b) Crane angle representation

**Figure 5.16:** Crane angle

## 5.6.2 Slider Joints

This section presents the sensor results for the 8 slider joints of the model.

### Linear displacement

The plot in **Figure 5.17** represents the displacement of the 8 links along the kinematic simulation.

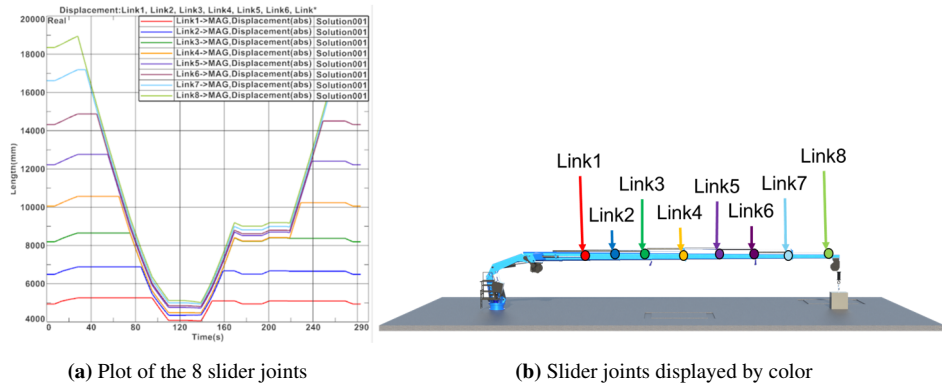


**Figure 5.17:** Linear displacement test for the slider joints

### Force in the slider joints

This test plots the force in the 8 slider joints, shown in **Figure 5.18**.

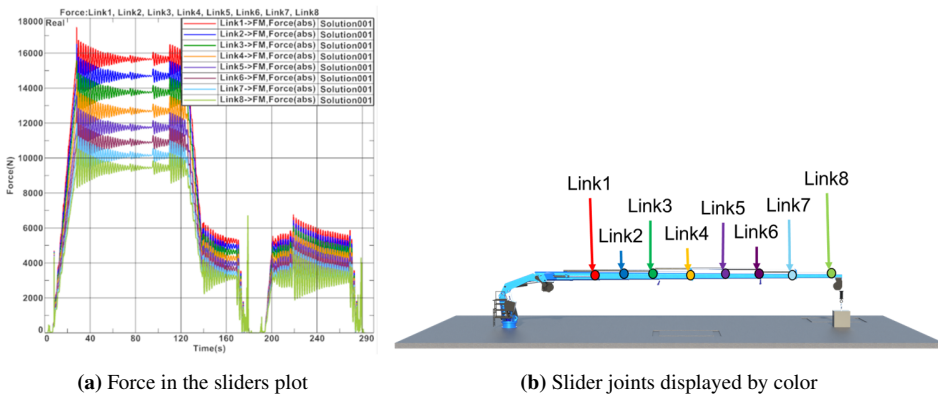


**Figure 5.18:** Force plot for the slider joints

### 5.6.3 Load and Hook sensors

In this section, the sensors located in the ending part of the crane are tested.

#### Linear displacement in the load and last link

This test plots two sensors to obtain the *end effector* position, displayed in **Figure 5.19**.

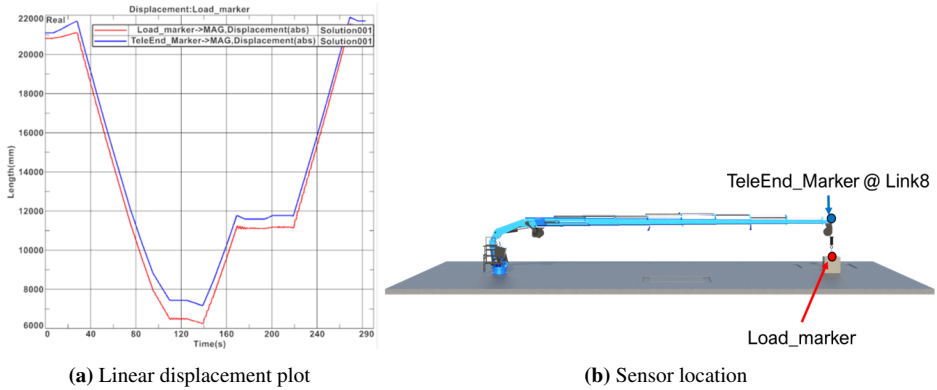


**Figure 5.19:** End effector position plot

#### Hook cable displacement

This test plots the displacement of the hook wire, displayed in **Figure 5.20**.

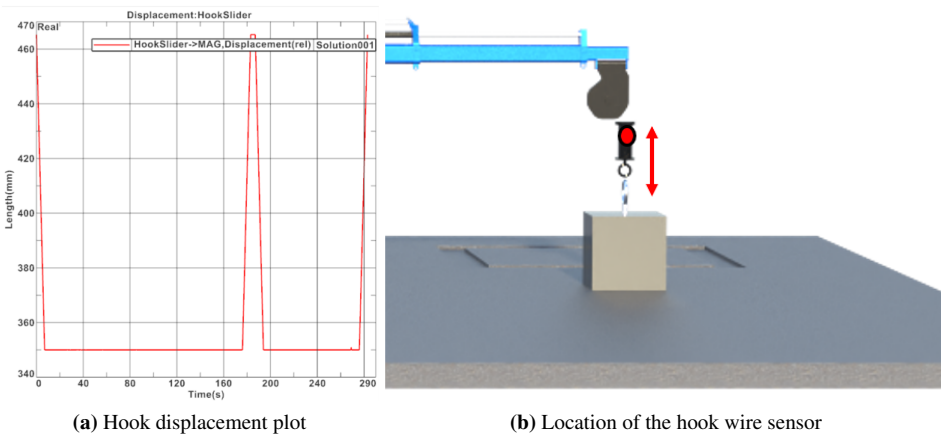


**Figure 5.20:** Hook cable displacement

### 5.6.4 Cylinders

In this section, the force in the revolute joints was plotted and assumed to be the forces acting on the cylinders, in **Figure 5.21**.

#### Forces in the rotational joints

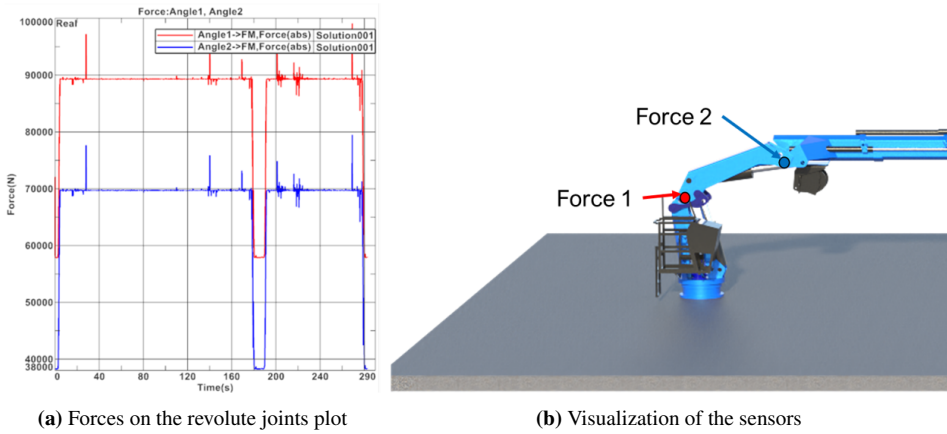


**Figure 5.21:** Forces in the revolute angles, also considered as forces in the cylinders

### 5.6.5 Motion Envelope

In **Figure 5.22**, a motion envelope plot was created to visualize all the positions where the crane passes by. This type of plot is useful for increasing the safety of the operations.

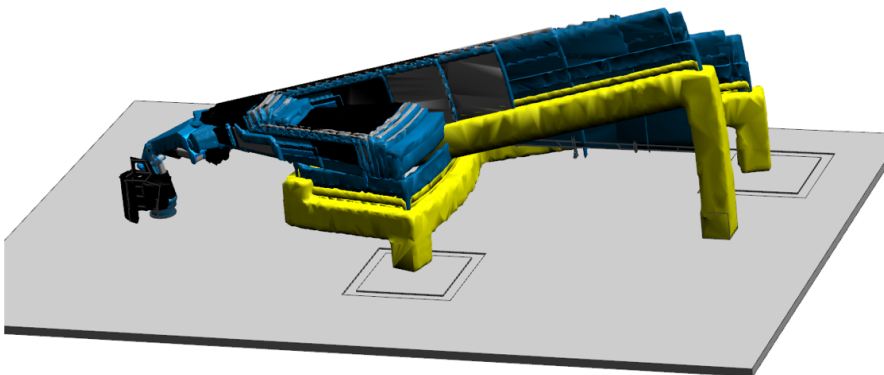


**Figure 5.22:** Motion envelope of the kinematic simulation





# Chapter 6

## Digital Twin

In this section, the assembly of the structural and kinematic simulations will be developed. The NX module used for this task is still NX Motion, with a different strategy for the structural analysis: an option for including a Flexible-Body during the motion simulations.

### 6.1 Connecting the structural and kinematic simulations

The model that will be used as the digital twin is the final kinematic simulation, since it has all the motion, joints, drivers, data inputs and outputs ready; and it is able to handle finite element models running in-real-time. In the structural simulation section 4.7, the flexible body simulation was built and solved with the purpose of adding it to the Digital Twin model.

The first step for merging the two models, is to select the option in the NX Motion module called *Flexible Body*, and select the part that was simulated, in this case was part number 3, or *PitchLink1* and load the test results gathered from the structural simulation. It is important to review that the part is assembled properly, and has set correctly the connections with the other parts.

When the part is loaded, the simulation can be solved. It will take more time than the kinematic simulation. As an observation, initially the simulation had quite high computation times, but when analyzed, the solution was to lower the weight of the box. With this improvement, the simulation runs smoothly. The cause of this problem might have been that the crane was not able to carry such load in the current conditions.

## 6.2 Results

When the model is solved, the simulation will change in several ways. The first change is that there is a structural analysis part that is constantly reacting according to the loads that the crane receives, and some components start oscillating. This happens due to the flexibility of the part because the displacement value is considered for the kinematic simulation. Several structural results can be plotted in the flexible body model, such as the displacement and the stress.

### 6.2.1 Displacement

In the following section, two displacement screenshots from the digital twin simulation will be compared.

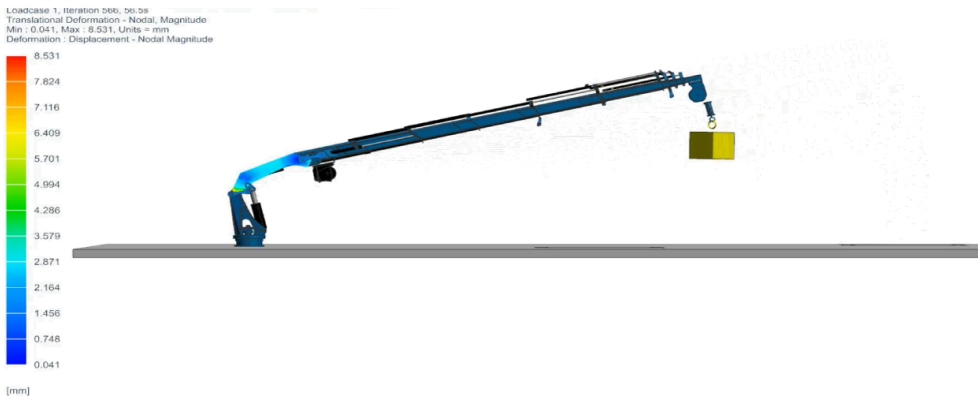


**Figure 6.1:** Screenshot of the Digital Twin simulation visualizing the displacement at 56 seconds

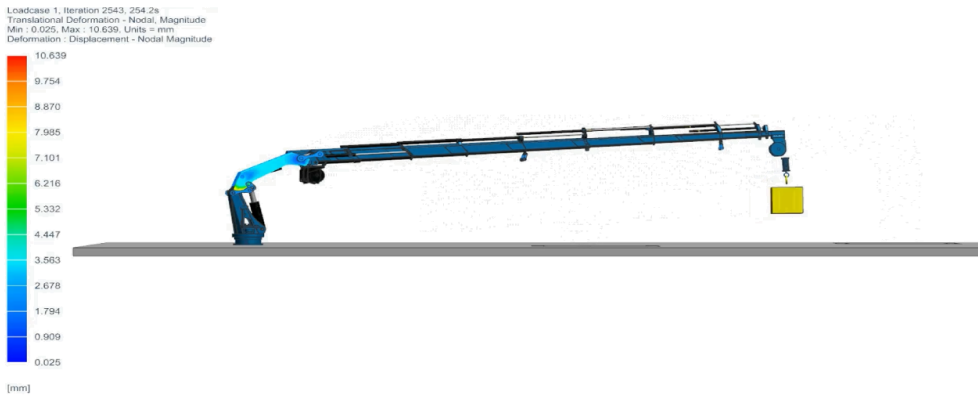


**Figure 6.2:** Screenshot of the Digital Twin simulation visualizing the displacement at 254 seconds

**Figure 6.1** shows the maximum displacement to be 8.531 millimeters at 56 seconds while **Figure 6.2** shows a maximum value of 10.369 millimeters at 254 seconds. This basic comparison shows how the digital twin simulation works. The values are updated constantly according to the loads that the model is receiving from all the motion bodies and joints setup.

## 6.2.2 Stress

For this simulation, a specific legend of results was applied to the stress plot, where the maximum value was set as 350 MPa, so the color variation was steady.

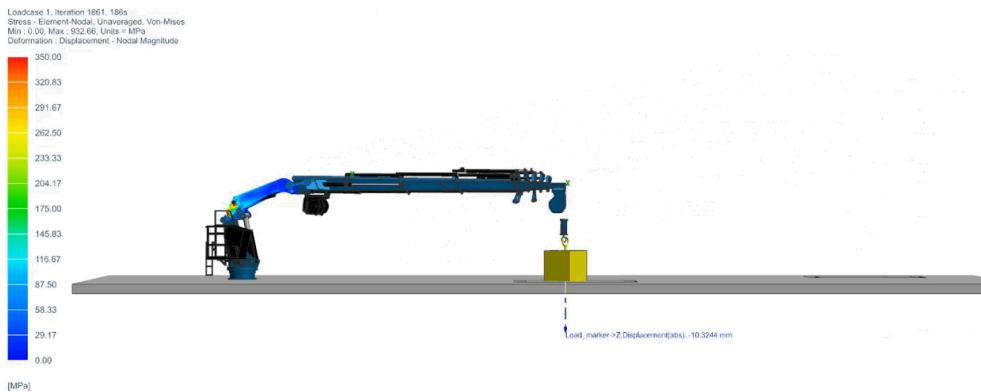


**Figure 6.3:** Screenshot of the Digital Twin simulation visualizing stress at 186s

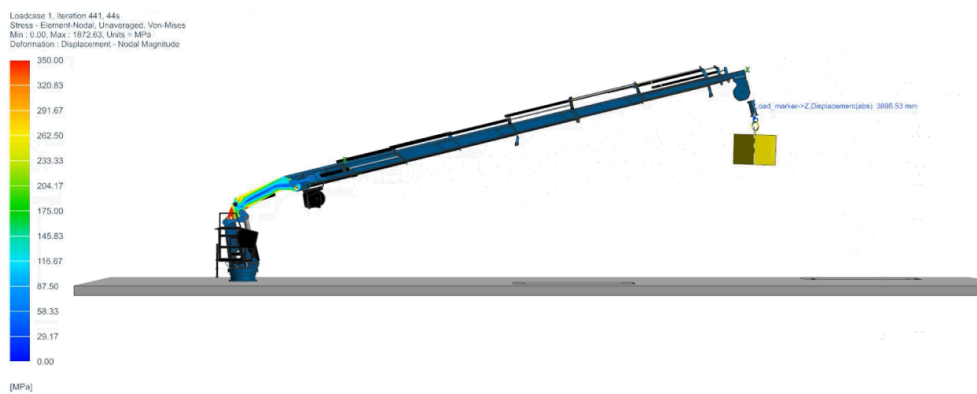


**Figure 6.4:** Screenshot of the Digital Twin simulation visualizing stress at 441s

An important event that was programmed in the kinematic simulation, was the loading and unloading of the box to show the impact in the structure. **Figure 6.3** shows the stress at 186 seconds, where the load is in the ground and as observed, the structural part is almost

completely at its lowest values. In contrast, **Figure 6.4** shows the stress at 441 seconds and presents a combination of colors.

This type of digital twin visualization where the kinematics and the structural analysis are offering a preview on how the loads will impact the crane open a wide set of possibilities for structural monitoring, smart controller feedback, predictive maintenance and decision support systems.

### 6.3 Smart Controller

This section explores the possibilities of designing a smart controller, or as named in **Figure 6.5**, a control output that is able to protect the crane operations and safety. As mentioned at the beginning of this project, a Digital Twin is defined as a closed loop system between a physical product and a virtual model. This closed loop represents the data gathered from the sensors mounted in the physical product, which serve as input for the virtual model. The virtual model evaluates the current and future scenarios, providing a control output or feedback signal.

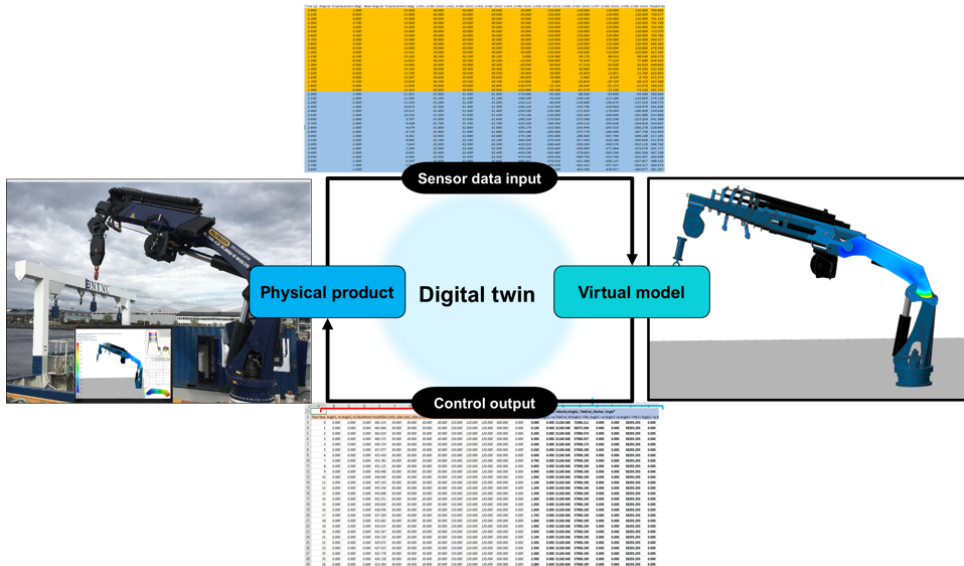


**Figure 6.5:** Digital Twin defining the sensor data input and control output

The control output already contains 50 data-sets gathered from the sensors in the virtual model, which were calculated based on the sensor data input. In order to convert this control output into a smart controller, a set of operational limits need to be defined to protect the crane operation and its crew. As an example, the controller output data measures the

force reaction in the joints, where the simulated value is above the suggested forces. The controller output must be able to limit the movement that would cause those forces, preventing the equipment damage.

In addition, by obtaining the sensor data input, the virtual model is able to monitor the status of the system, and in case there is a reading that is out of the usual values, an alert will be sent to the user for maintenance or at least inspection. This allows the implementation of condition-based predictive maintenance.



## Further work

As displayed in **Figure 7.1**, the digital twin goal is to be able to simulate and visualize the crane operations while providing structural monitoring and reducing maintenance costs. Considering the development reached in this project, the digital twin has already been designed and tested using simulation data. The next step is to close the loop, by setting the physical connection between the crane and the virtual models.

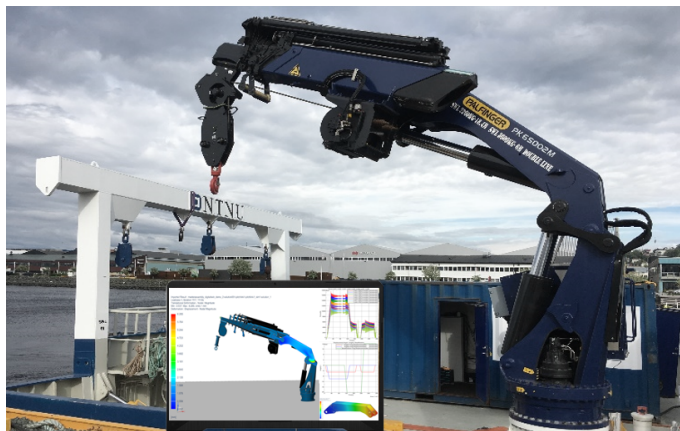


**Figure 7.1:** Goal of the digital twin for the maritime crane

Several tasks have been identified as further work for the structural, kinematic and digital twin simulations in order to improve the accuracy and reduce the simulation time.

For the structural simulations, the 1D model simplification was identified as having a high potential of running in real time, therefore it requires refinement in order to reduce the variation in the displacement, which currently is 14%. In addition, to reduce the simula-

tion time by eliminating the need for the revolute and slider joints, a one-body 3D model can be developed, testing the complete model as a rigid structure. This model can also be tested for a mesh convergence in a faster way, since it consists only of one solid body. Another task for reducing the simulation time, is to use the one-body 3D model to develop a 2D-Shell model and evaluate its behavior, since it is well-known that 3D elements increase the simulation time, and 2D shell models provide a positive balance between accuracy and efficiency.

As further work for the kinematic simulation, it could be valuable to add more detailed parameters to the hydraulic cylinders and use them for the crane control. In addition, the crane hook slider joint can be modified to provide a more accurate motion using a spherical joint. To reduce the simulation time, a joint-by-joint test can be run, to find the joint that takes a higher time to simulate and improve it. Finally, the ship motions can be added to the simulation.

For the digital twin model, the flexible body option can be tested for all the parts, and use the sensor plots to compare its behavior with the kinematic simulation. The most valuable further work task is to connect the digital twin to the physical sensors in the crane and test the accuracy of the simulations.



## Conclusions

In this project, the use of the digital twin was explored and applied to a maritime crane to perform structural monitoring and predictive maintenance using Siemens NX. As noted in the state of the art section, these topics are still on the research phase, reporting very few successful applications. Therefore this project represents one of the first attempts of mixing the topics of digital twin, maritime cranes, structural monitoring and predictive maintenance.

For the development of this project, several computational methods were used to create a digital twin for a maritime crane. The structural simulation was developed using NX FEA and NX Sim, while the kinematic simulation used NX Motion. As observed in the structural simulation chapter, the 3D elements simulation provide accurate results while sacrificing the ability to run in real time connected to a digital twin. Therefore, several simplifications were developed and tested to evaluate the possibility of running in real time and providing accurate results, such as the idealized model and the 1D beam tests. The balance between accuracy and computational efficiency can be improved by continuing the iterations applying the simulation-based design method to test different model simplifications and strategies, and applying the lessons learned to the next iteration, in addition to a set of mesh convergence tests. Simulation-based design was also used to find the optimal sensor placement together with the structural simulations, creating an iterative process that allowed the identification of high-stress zones.

The data required for designing a smart controller is the definition of the crane safety operation zones and loads, and to define what type of feedback will be applied to the crane. If it would be used as input directly by the crane, or it will be an alarm for the operator. NX can be used for developing digital twins, due to its capacity of merging the structural and kinematic models. Obtaining an accurate and efficient model is essential for simulating real-time data. The digital twin simulation developed opens the possibilities to condition-based predictive maintenance, structure monitoring and decision-support systems.



# References

- [1] Palfinger, “PK 65002 SH High Performance,” 2020.
- [2] L. Bjørn, “NTNU students build Digital Twin of RV Gunnerus during summer project,” 2018.
- [3] Siemens Software, “Simcenter: Modelling the digital twin of an aircraft fuel system,” 2020.
- [4] B.-J. Zhang and S.-L. Zhang, *Research on Ship Design and Optimization Based on Simulation-Based Design (SBD) Technique*. Springer, 2019.
- [5] M. Ben-Daya, S. Duffuaa, A. Raouf, J. Knezevic, and D. Ait-Kadi, *Handbook of Maintenance Management and Engineering*. Springer, 2009.
- [6] J. Kim, M.H ; Lee, “Sensing solutions for assessing and monitoring offshore structures,” *Elsevier Sensor Technologies for Civil Infrastructures*, vol. 2, pp. 550–564, 2014.
- [7] Y. Fujino, D. Siringoringo, Y. Ikeda, T. Nagayama, and T. Mizutani, “Research and Implementations of Structural Monitoring for Bridges and Buildings in Japan,” *Elsevier Engineering*, vol. 5, no. 6, pp. 1093–1119, 2019.
- [8] E. Negri, L. Fumagalli, and M. Macchi, “A review of the roles of Digital Twin in CPS-based production systems,” *Elsevier Procedia Manufacturing*, vol. 11, pp. 939–948, 2017.
- [9] C. Villarreal, “Literature Review on Cyber-Physical Systems Design,” *Elsevier Procedia Manufacturing*, vol. 45, pp. 295–300, 2020.
- [10] Arrowhead Project, “Arrowhead framework,” 2019.
- [11] E. Glaessgen and D. Stargel, “The Digital Twin Paradigm for Future NASA and U.S. Air Force Vehicles,” 2012.
- [12] Siemens, “Digital twin,” 2017.

- 
- [13] S. Haag and R. Anderl, "Digital twin - proof of concept," *Elsevier Manufacturing Letters*, vol. 15, no. 4, pp. 64–66, 2018.
- [14] R. Rosen, G. Von Wichert, G. Lo, and K. Bettenhausen, "About the importance of Autonomy and Digital Twins for the Future of Manufacturing," *Elsevier IFAC-PapersOnLine*, vol. 48, pp. 567–572, 2015.
- [15] F. Tao, J. Cheng, Q. Qi, and M. Zhang, "Digital twin-driven product design, manufacturing and service with big data," *Springer International Journal of Advanced Manufacturing Technology*, 2018.
- [16] Offshore Simulator Centre, "Training personnel," 2019.
- [17] T. Uhlemann, C. Schock, C. Lehmann, S. Freiberger, and R. Steinhilper, "The Digital Twin: Demonstrating the potential of real time data acquisition in production systems," *Elsevier Procedia Manufacturing*, vol. 9, pp. 113–120, 2017.
- [18] W. Mefteh, "Simulation-Based Design: Overview about related works," *Elsevier Mathematics and Computers in Simulation*, vol. 152, pp. 81–97, 2018.
- [19] C. Yang and F. Huang, "An Overview of Simulation-Based Hydrodynamic Design of Ship Hull Forms," *Elsevier Journal of Hydrodynamics*, vol. 28, no. 6, pp. 947–960, 2016.
- [20] X. Han and J. Liu, *Numerical Simulation-based Design: Theory and Methods*. Springer, 2020.
- [21] O. Jaewon, M. Cheonhong, C. Sugil, B. Daesung, and K. Hyungwoo, "Concept of an advanced simulation-based design for engineering support of offshore plant equipment industries and its realization method," *Elsevier Ocean Engineering*, vol. 121, pp. 369–381, 2016.
- [22] M. Bossak, "Simulation based design," *Elsevier Materials Processing Technology*, vol. 76, pp. 8–11, 1998.
- [23] X. Telleria, D. Ugarte, J. Esnarola, M. Ezkurra, and L. Colomo, "Automation of Simulation Based Design Validation and Reporting of a Valve Family," *Elsevier Procedia CIRP*, vol. 84, pp. 986–991, 2019.
- [24] P. Goncharov, I. Artamonov, T. Khalitov, S. Denisikhin, and D. Sotnik, *Engineering Analysis with NX Advanced Simulation*. Siemens PLM, 2014.
- [25] C. Kuang-Hua, "Structural analysis," *Elsevier Product Performance Evaluation with CAD/CAE*, pp. 43–119, 2013.
- [26] B. Yong and W. Jin, "Wave Loads for Ship Design and Classification - Marine Structural Design," *Elsevier Marine Structural Design*, vol. 2, pp. 73–93, 2016.
- [27] E. Oñate, *Structural Analysis with the Finite Element Method: Linear Statics*, vol. 1: Basis and Solids. Springer, 2009.

- 
- [28] E. Oñate, *Structural Analysis with the Finite Element Method: Linear Statics*, vol. 2: Beams, Plates and Shells. Springer, 2013.
- [29] A. Hamdan, M. Sultan, and F. Mustapha, “Structural health monitoring of biocomposites, fibre-reinforced composites, and hybrid composite,” *Elsevier Composites Science and Engineering*, pp. 227–242, 2019.
- [30] A. Jiménez-Sánchez, G. Silva-Navarro, and F. Beltrán-Carbajal, “Structural Analysis of Superficial Cracks on Structural Elements,” *IEEE International Conference on Electrical Engineering, Computing Science and Automatic Control*, 2019.
- [31] Encyclopædia Britannica, “Anemometer,” 2020.
- [32] Incorporated Research Institutions for Seismology, “What is a seismometer?,” 2020.
- [33] A. Fernández and D. Dang, *Getting Started with the MSP430 Launchpad*. Elsevier, Newnes, 2013.
- [34] Keyence, “What are displacement gauges?,” 2020.
- [35] Omega Engineering, “Strain gauge,” 2020.

---

# Appendix

## 8.1 Structural Simulation with 5 kN

This appendix section displays the structural simulation results for the cases with 5 kN. To see the results with 20 kN, see section 4.4.1.

### 8.1.1 3D Partial Test

This section shows the results for the partial test using 5 kN, both for the real and idealized model.

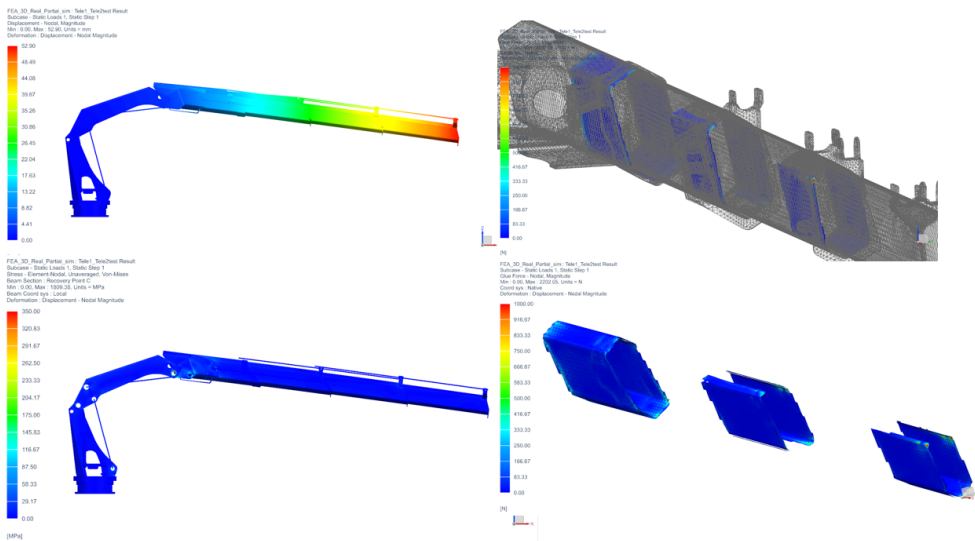
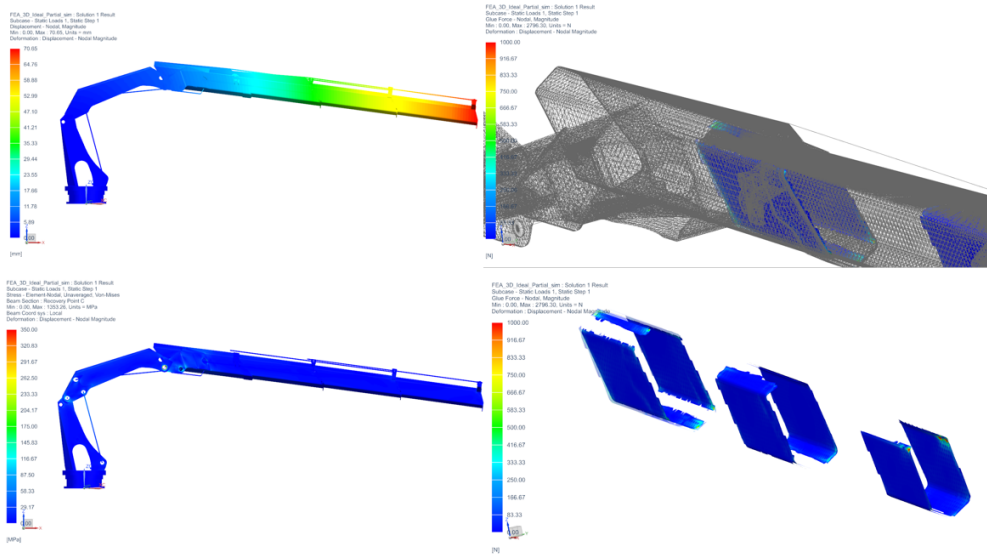


Figure 8.1: 3D Real Model - Partial Test at 5 kN result

As observed in the **Table 8.1**, the ideal model reduces the simulation time, but adds variation in the displacement values.



**Figure 8.2:** 3D Ideal Model - Partial Test at 5 kN result

Test number	Model configuration	Simulation Time [s]	Displacement [mm]
1	Real partial	900	52.90
2	Ideal partial	720	70.65

**Table 8.1:** Results for 3D partial tests at 5 kN





Test number	Model configuration	Simulation Time [s]	Displacement [mm]
1	Real complete	10800	362.26
2	Ideal complete	6300	382.49

**Table 8.2:** Results for 3D complete tests at 5 kN

### 8.1.3 1D Square cross-section test

This section tests the square cross-section with a load of 5 kN.

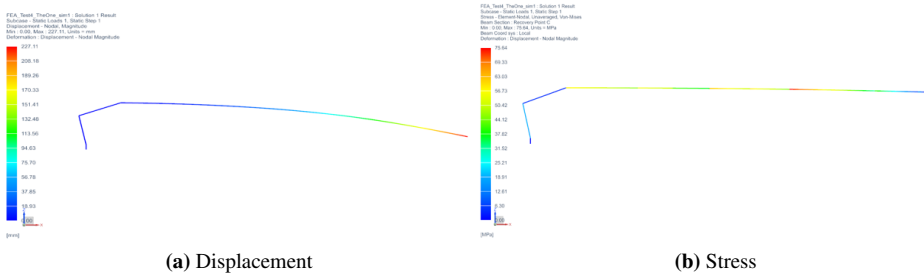


**Figure 8.5:** 1D square cross-section approximation test results at 5 kN

### 8.1.4 1D Real cross-section test

This model tests the 1D beam model with the real cross-section and a load of 5 kN.

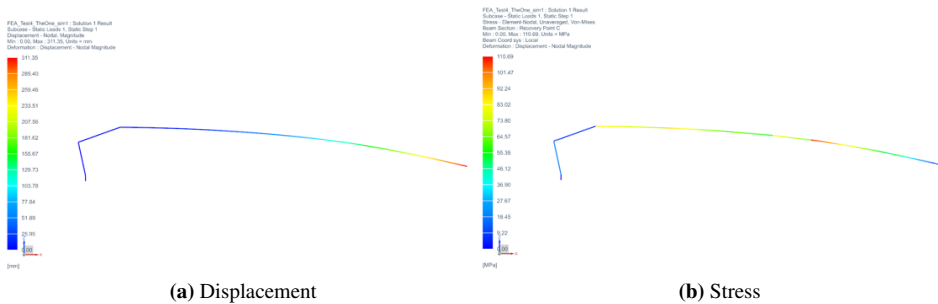


**Figure 8.6:** 1D real cross-section approximation test results at 5 kN

## 8.1.5 Results

The summary of results for the complete testing serie of 5 kN is displayed in **Table 8.3**. For the result summary of 20 kN, see section 4.5. As observed in the results summary, the idealized model reduces the simulation time in a 20% to 42% but it adds considerable variation in the displacement from 6% to 33%. For the 1D beam models, the simulation is reduced by 99% and the variation regarding the displacement value of the real cross-section model was 14%.

Test	Model	Configuration	Displacement [mm]	Simulation time [s]
1	3D Partial	Real	52.90	900
		Idealized	70.65 ↑ 33%	720 ↓ 20%
2	3D Complete	Real	362.26	10800 *
		Idealized	382.49 ↑ 6%	6300 ↓ 42%
3	1D Complete	Square	227.11 ↓ 37%	0.5 ↓ 99%
		Real	311.35 ↓ 14%	0.5 ↓ 99% *

**Table 8.3:** Structural simulation test results summary for 5 kN

## 8.2 Kinematic Simulation

### 8.2.1 List of sensors

The list of sensors is divided into revolute, slider joints and additional sensors.

Part	Input variable	Measurement	Output name in excel and NX Plot
1	<b>Angle1</b>	Angular displacement	Angle1 → ang,Displacement(abs)
2		Force	Angle1 → FM,Force(abs)
3		Velocity	Angle1 → angd,Velocity(abs)
4	<b>Angle2</b>	Angular displacement	Angle2 → ang,Displacement(abs)
5		Force	Angle2 → FM,Force(abs)
6		Velocity	Angle2 → angd,Velocity(abs)
7	<b>BaseRotation</b>	Angular displacement	BaseRotation → ang,Displacement(abs)
8		Force	BaseRotation → FM,Force(abs)
9		Velocity	BaseRotation → angd,Velocity(abs)

**Table 8.4:** List of sensors and plots for the revolute joints

Part	Input variable	Measurement	Output name in excel and NX Plot
10	<b>Link1</b>	Displacement	Link1 → MAG,Displacement(abs)
11		Position	Link1 → pos,Displacement(abs)
12		Velocity	Link1 → posd,Velocity(abs)
13		Force	Link1 → FM,Force(abs)
14	<b>Link2</b>	Displacement	Link2 → MAG,Displacement(abs)
15		Position	Link2 → pos,Displacement(abs)
16		Velocity	Link2 → posd,Velocity(abs)
17		Force	Link2 → FM,Force(abs)
18	<b>Link3</b>	Displacement	Link3 → MAG,Displacement(abs)
19		Position	Link3 → pos,Displacement(abs)
20		Velocity	Link3 → posd,Velocity(abs)
21		Force	Link3 → FM,Force(abs)
22	<b>Link4</b>	Displacement	Link4 → MAG,Displacement(abs)
23		Position	Link4 → pos,Displacement(abs)
24		Velocity	Link4 → posd,Velocity(abs)
25		Force	Link4 → FM,Force(abs)
26	<b>Link5</b>	Displacement	Link5 → MAG,Displacement(abs)
27		Position	Link5 → pos,Displacement(abs)
28		Velocity	Link5 → posd,Velocity(abs)
29		Force	Link5 → FM,Force(abs)
30	<b>Link6</b>	Displacement	Link6 → MAG,Displacement(abs)
31		Position	Link6 → pos,Displacement(abs)
32		Velocity	Link6 → posd,Velocity(abs)
33		Force	Link6 → FM,Force(abs)
34	<b>Link7</b>	Displacement	Link7 → MAG,Displacement(abs)
35		Position	Link7 → pos,Displacement(abs)
36		Velocity	Link7 → posd,Velocity(abs)
37		Force	Link7 → FM,Force(abs)
38	<b>Link8</b>	Displacement	Link8 → MAG,Displacement(abs)
39		Position	Link8 → pos,Displacement(abs)
40		Velocity	Link8 → posd,Velocity(abs)
41		Force	Link8 → FM,Force(abs)
42		Angular displacement	Link8 → Euler2,Displacement(abs)

**Table 8.5:** List of sensors and plots for the slider joints

---

Part	Input variable	Measurement	Output name in excel and NX Plot
43		Load pos. in Z	Load-marker → Z,Disp.(abs)
44	<b><i>Load-marker</i></b>	Load velocity	Load-marker → MAG,Velocity(abs)
45		Load disp.	Load-marker → MAG,Disp.(abs)
46	<b><i>Cylinder1-marker</i></b>	Cylinder disp.	Cylinder1-Marker → MAG,Disp.(abs)
47	<b><i>Cylinder2-marker</i></b>	Cylinder disp.	Cylinder2-Marker → MAG,Disp.(abs)
48	<b><i>HookSlider</i></b>	Hook position	HookSlider → pos,Disp.(abs)
49		Angular disp.	TeleEnd-marker → Euler2,Disp.(abs)
50	<b><i>TeleEnd-marker</i></b>	Displacement	TeleEnd-marker → MAG,Disp.(abs)

**Table 8.6:** List of sensors and plots for the additional sensors

